

Structural analysis and facies
distribution of Cryogenian glacial
rocks and regional structures in the
Willouran Ranges, SA

Thesis submitted in accordance with the requirements of the University of
Adelaide for an Honours Degree in Geology

Sameh Shahin
November 2016



THE UNIVERSITY
of ADELAIDE

**STRUCTURAL ANALYSIS AND FACIES DISTRIBUTION OF CRYOGENIAN
GLACIAL ROCKS AND REGIONAL STRUCTURES IN THE WILLOURAN RANGES,
SA**

RUNNING TITLE: NEOPROTEROZOIC GEOLOGY OF TERMINATION VALLEY

ABSTRACT

The Willouran Ranges lie at the far NW extremity of the Flinders Ranges, on a NW-SE fault-bound trend with the Peake and Denison Ranges along strike to the NW, and the Olympic Domain of the Gawler Craton on the footwall to the west. The range is formed from a near-continuous sequence of Adelaidean Neoproterozoic sedimentary and volcanic rocks, and is cut by two major fault systems. The lower part of the Adelaidean succession is particularly well exposed in the region, including a Sturtian (ca. 720-660 Ma) aged glacial deposit, the Bolla Bollana Formation. This formation is a glacial deposit thought to be deposited from the oldest Cryogenian global glaciation event.

The study will present new maps of Termination Valley, presented alongside cross-sections outlining major structures in the area, and sedimentary logs characterising the glacial diamictite deposits. Detrital Zircon dates obtained from the study outline radiometric U-Pb data corresponding to the maximum age of deposition of the Bolla Bollana Tillite Formation and overlying Tapley Hill Formation, with ages corresponding to 673 ± 19 Ma and 654 ± 13 Ma respectively. In addition to providing Australia's first informative U-Pb radiometric age constraint on a Sturtian Tillite facies, the study will discuss the provenance of the sediments using multi-dimensional scaling techniques, and provide evidence for extensive north and west extending continental ice sheets.

KEYWORDS

Structure; Willouran Ranges; Northern Flinders Ranges; Neoproterozoic; Sturtian; Geochronology; Diamictite; Umberatana Group; Zircon; Bolla Bollana Formation; Tapley Hill Formation; Burra Group

Contents

Structural Analysis and Facies Distribution of Cryogenian Glacial Rocks and Regional Structures in The Willouran Ranges, SA	i
Running Title: Neoproterozoic Geology of Termination Valley	i
Abstract.....	i
Keywords.....	i
List of figures and tables	iv
1 Introduction	1
2 Geological Setting	2
2.1 Adelaide Rift Complex.....	2
2.2 Northern Flinders Ranges & Willouran Ranges.....	2
2.3 Termination Valley.....	3
2.3.1 Burra Group	3
2.3.2 Umberatana Group.....	4
3 Methodology	5
3.1 Geochronology	5
3.2 Structural Mapping	7
3.3 Cross sections	8
3.4 Sedimentology.....	8
4 Observations and Results	8
4.1 Geological Map and Cross Sections.....	8
4.2 Structural Facies Analysis	15
4.2.1 Regional structure and deformation.....	15
4.2.2 Termination Valley D1	15
4.2.3 Fold description	17
4.3 Subarea Analysis	18
4.3.1 Subarea 1.....	18
4.3.2 Subarea 2.....	18
4.3.3 Subarea 3.....	19
4.3.4 Subarea 4.....	19
4.4 Sedimentology.....	22
4.4.1 Bolla Bollana Formation.....	22
4.4.1.1 Matrix Supported Conglomerate (MSC) Facies.....	26
4.4.1.2 Grain Supported Conglomerate (GSC) Facies	26
4.4.1.3 Shale Facies.....	27
4.4.1.4 Dolomite Facies.....	27

4.4.1.5	Pelletal Magnesite Facies	27
4.5	Geochronology	27
4.5.1	Sample W16-06	29
4.5.2	Sample W16-07	29
4.5.3	Sample W16-08	29
4.5.4	Sample W16-09	30
4.5.5	Sample W16-10	30
4.6	Age of deposition	38
4.7	Provenance.....	38
5	Discussion	44
5.1	Depositional Environment of the Lower Umberatana Group:	44
5.2	Chronology of Cryogenian Glaciation	45
5.3	Detailed Analysis of Detrital Zircon signature and implications for provenance	46
5.3.1	Major Peaks	46
5.3.2	Minor Peaks	47
6	Conclusion.....	51
7	Acknowledgments.....	52
8	References	53
9.1	Appendix A: Structural Data	57
9.2	Appendix B: Geochronology:.....	73

LIST OF FIGURES AND TABLES

Figure 1: Geological Map of termination Valley as mapped in field.....	10
Figure 2 Younging direction indicators. a/b) low angle cross beds in sandstones located in the Copley Quartzite Formation, c) Stromatolite mounds with 2 different cross sections, arrows imply younging direction, located in the Skillogalee Dolomite Formation	11
Figure 3: Vertical cross-section along transect A-A' Note: Cross section reconstruction is modelled on interpreted geology prior to erosion.....	13
Figure 4: Vertical cross-section along transect B-B' Note: Cross section reconstruction is modelled on interpreted geology prior to erosion.....	14
Figure 5: Stereonet of all structural data taken in field. Point “3” represents average pole to best fit plane of data. Red contour areas represent highest density of structural measurements and blue/white the least dense. Overall Structural trend of folds from total data represents a NW, moderately plunging folds.....	16
Figure 6: Geological map of Termination Valley with coloured boxes representing the groups of structural measurements that define each sub area analysis. Pink box=subarea 1, dark blue box=subarea 2, cyan box= subarea 3, red box=subarea 4.	20
Figure 7: Stereographic projections for each subarea group, a) subarea 1, b) subarea 2, c) subarea 3, d) subarea 4	21
Figure 8: Representative diamictite facies within the Bolla Bollana Tillite Formation .	23
Figure 9: Sedimentary Log of Bolla Bollana Formation, taken from first Bolla Bollana Formation where in contact with the Burra Group rocks of Termination Valley.	24
Figure 10: Representative detrital zircons from field samples (imaged under cathodoluminescence)	32
Figure 11: U-Pb zircon age Concordia plots ($\pm 10\%$ concordance). a) W16-06 concordia plot ai) W16-06 main age population b) W16-07 concordia plot bi) W16-07 main age population c) W16-08 concordia plot ci) W16-08 main age population.....	36
Figure 12: Multi-Dimensional Scaling plot of all field samples and 3 hypothesised proximal provinces (Gawler Craton, Musgrave Block and Curnamona Craton)	40
Figure 13: Kernel Density Estimate Plots of all samples	42
Figure 14: Probability density function plot for detrital zircon U-Pb ages. Plots on right represent samples taken from field area, Left represents Elatina Formation (post Umberatana deposit, modified from (Rose et al., 2013) and Burra Group (pre Umberatana deposit), modified from (Mackay, 2011)	43
Figure 15: Cratonic Australia, with particular reference to possible provenance sources to the Willouran trough	50
Table 1: Termination Valley formation key features	22
Table 2: Lithofacies Summary of individual beds mapped in Sedimentary Log (Figure 9) of Bolla Bollana Tillite Formation	25
Table 3: Zircon descriptions, sample W16-06.....	33
Table 4: Youngest Detrital Zircon summary	38
Table 5: Major and minor age peaks present in Kernel Density Estimate Plots	41
Table 6: Major and minor age peaks present in Probability Density Function Plots	42
Table 7: Structural bedding readings and locations.....	57
Table 8: Lineation readings	65
Table 9: Slicken line readings	65

Table 10: Subarea 1 readings	65
Table 11: Subarea 2 readings	66
Table 12: Subarea 3 readings	70
Table 13: Subarea 4 readings	71
Table 14: U-Pb data sample W16-06	73
Table 15: U-Pb data sample W16-07	77
Table 16: U-Pb data sample W16-08	78
Table 17: U-Pb data sample W16-09	82
Table 18: U-Pb data sample W16-10	85
Table 19: Gawler Craton provenance data	89
Table 20: Musgrave Block provenance data	105
Table 21: Curnamona Craton provenance data	112

1 INTRODUCTION

The Cryogenian (ca. 720-635 Ma) was arguably host to at least two of the most extreme ice ages known in the last two billion years. Remnant glacially derived strata record evidence for these extreme climatic conditions and their existence on a global scale (Hoffman et al., 1998; Kirschvink, 1992). The Willouran Ranges are host to well exposed Neoproterozoic strata, including Sturtian (ca. 720-660 Ma) aged glacial deposits correlated to the older of these two extreme ice age events. The Willouran Ranges preserve a detailed record of Earth's continental development, in particular the breakup of super continent Rodinia and later formation of Gondwana. Evidence for these large scale events is recorded in the sedimentology of the stratigraphy and its structural deformation.

Absence of radiometric age constraints on Sturtian and Marinoan glacial deposits across the globe has contributed to uncertainty in the age, synchronicity and extent of Neoproterozoic glacial events (Allen & Etienne, 2008). Depositional age constraints on Sturtian and Marinoan glacial deposits in the Adelaide Rift Complex (ARC) are represented by age's correlative with Re-Os ages of overlying strata. To better understand the source and timing of these deposits, LA-ICP-MS dating will be conducted on detrital zircons from samples within Termination Valley, a well exposed section of the Willouran Ranges. The ambiguity in the nature of the glacial deposits of Termination Valley will be resolved with structural mapping of the area and analysis of its sedimentology.

This paper will present a structural map and cross-sections of Termination Valley, and analysis of its sedimentology. It will also present new radiometric dates derived from a detailed detrital zircon study on the area, that include the first radiometric age constraints on Sturtian diamictites.

2 GEOLOGICAL SETTING

2.1 Adelaide Rift Complex

Intra-cratonic rifting in the Neoproterozoic was responsible for Australia detaching from Western Laurentia, and the beginning of many (possibly up to 5) rift phases (Preiss, 2000). As a result a super basin complex developed, known as the Adelaide Rift Complex also known as the Adelaide Geosyncline (Sprigg, 1952).

The strata and deformation of the Adelaide Rift Complex records evidence for its involvement in supercontinent Rodinia's break up at ca. 830 Ma (Li et al., 2003; Preiss, 2000), where it was attached to Laurentia, until its final basin inversion during the Cambrian Ordovician Delamerian Orogeny at ~527 Ma (Mackay, 2011)

2.2 Northern Flinders Ranges & Willouran Ranges

The Northern Flinders Ranges connect to the Willouran Ranges in a north-western extension (Hearon et al., 2015). Stratigraphy in both areas are very similar, as both maintain records of early Adelaidean rocks, primarily the Warrina Supergroup (including the oldest Callana Group) and the Heysen Supergroup (including Sturtian and Marinoan glacial deposits). The Warrina Supergroup represent initial stages of

intracontinental rifting of Australia, while the Heysen Supergroup represents development of a passive margin between Australia and Laurentia (Powell et al., 1994).

2.3 Termination Valley

2.3.1 Burra Group

The Burra Group consists of four subgroups; Emeroo, Mundallio (Skillogalee Dolomite), Bungarider and Belair Subgroup. The Copley Quartzite Formation and Skillogalee Formation belong to the Emeroo and Mundallio Subgroups respectively within Termination Valley. These formations are particularly well exposed along the eastern limb of a major syncline.

The Burra Group rocks in the area reflect gradual basin deepening associated with extension of a rift margin between Australia and Laurentia. The Copley Quartzite Formation is a quartz rich, siliciclastic subgroup. It contains sandstone dominated layers and sedimentary structures, which show a progression from a fluvial to deltaic setting. Younger in age, the Skillogalee Dolomite Formation reflects a marginal to shallow marine setting. Towards the Burra-Umberatana contact, the strata contains thick stromatolitic carbonates, siltstones and shale. This provides evidence for marine transgression and a change in the environmental setting.

The Boucaut Volcanics are a bimodal suite of basalt and rhyolitic ignimbrite (Forbes, 1977) interbedded with basal Burra Group rocks. These ignimbrites are located in several areas within the ARC, but most notably in the Nackara Arc where the rhyolitic

beds have been dated and yield U-Pb SHRIMP zircon ages of 777 ± 7 Ma, defining the maximum age of the Burra Group (Preiss, 2000).

The Rook Tuff located within the underlying Callana beds yields a SHRIMP U-Pb age of 802 ± 10 Ma from zircons in a lenticular porphyritic dacite from within the Rook Tuff, also representing the possible maximum age of the Burra Group. The lower extent of the Burra Group is poorly constrained, with a maximum age of deposition for the youngest rocks given according to correlation dates of first Cryogenian glacial rocks of Oman. These rocks are represented by a tuffaceous horizon found from the lowest glaciogenic unit in the Huqf Supergroup of Oman, dated at $723 +16 -10$ Ma (U-Pb zircon age, (Brasier et al., 2000)).

2.3.2 Umberatana Group

The Umberatana Group consists of four subgroups; Yudnamutana, Nepouie, Upalinna and the Yerelina Subgroup. The stratigraphy of the Umberatana Group relates to the Sturtian and Marinoan glacial events, which coincide with formation of a passive margin between Australia and Laurentia (Le Heron et al., 2011).

Outcropping Bolla Bollana Formation belonging to the Yudnamutana Subgroup rocks represent a glacial deposit with absence of defining sedimentary structures. The formation outcrops in several areas of the Northern Flinders Ranges, including a well exposed section in Mount Painter (Young & Gostin, 1989) that includes defining marine glacial rainout structures.

An exact geochronological age of the Umberatana Subgroup is a subject of scrutiny, due to the sparsity of dateable volcanic material in the Flinders Ranges that coincide with deposition of the Umberatana Group.

Geochronological analysis on equivalent rock groups in countries such as Oman, Mongolia, Canada and Zambia have yielded U-Pb zircons of age ~730-717 Ma for conformably overlying volcanic horizons (Brasier et al., 2000; Mahan et al., 2010; Rooney et al., 2015). In the Flinders ranges, the Tindelpina Shale formation, representative of a transgressive cycle proceeding deglaciation, has yielded a Re-Os age of ~643 Ma (Rooney et al., 2014; Rooney et al., 2015) and represents demise of Sturtian glaciation in the Central Flinders.

The age constraint of the Upper Umberatana Group is highly debated. Age estimates of cap carbonates belonging to the Yerelina Subgroup are put at ca. 635 Ma and currently signify the end of the Cryogenian period. Despite this, a U-Pb zircon age of 621 ± 7 Ma from a tuff directly above the cap carbonate of an Elatina Formation equivalent suggests a younger age (Zhang et al., 2005).

3 METHODOLOGY

3.1 Geochronology

Whole rock samples were taken from the field from a range of areas within Termination Valley, in an attempt to represent the Umberatana Subgroup as a whole (i.e. spaced along strike and down strike). Samples were cut with a diamond saw in order to expose fresh surfaces and remove any weathered faces before being crushed into coarse

fragments by a jaw crusher. The sample is then placed into a multi-layer sieve designed to separate the sample into $\leq 79\mu\text{m}$, $\geq 79\mu\text{m} - \leq 400\mu\text{m}$ and $\geq 400\mu\text{m}$ fractions. The sample is run through a ring mill multiple times to continually fine the large fragments and intermittently sieved to further separate the sample by size.

The $\geq 79\mu\text{m} - \leq 400\mu\text{m}$ sample fraction was panned in water to concentrate heavy minerals and remove lighter fractions, with the intent to concentrate heavy minerals in sample. The resulting heavy mineral fraction is dried before being run through a frantz magnetic separator to remove any magnetic minerals to concentrate zircons, a non-magnetic, U-Pb containing mineral.

Heavy liquid separation using a LST fast float heavy fluid was conducted with the heavy mineral fraction dropped into a column of the fluid, separating anything lighter than $2.8\text{g}/\text{cm}^3$ to the top of the column and anything heavier to the bottom. The heavy minerals on the bottom are frozen in place using dry ice, separated, washed and dried.

Zircons are then handpicked under a reflected light microscope, then mounted in epoxy resin and left to set. After the resin has solidified, the mounts are polished in order to expose the minerals. They are then imaged on a Qanta 600 SEM, using backscatter for general track reference images and, cathodoluminescence to identify ideal laser target spots and zircon morphology. It should be noted, mounts were not carbon coated due to technical problems and as such imaging was conducted under low vacuum conditions.

Zircons were ablated on a New Wave 213 - 7500cx ICP-MS (spot size $30\mu\text{m}$, 30 second background acquisition and 30 seconds data acquisition). Primary zircon standard GJ-1

and a secondary checking standard PLESOVICE were used at the LA-ICP-MS facility (Adelaide Microscopy).

GJ-1; known TIMS (Thermal Ionization Mass Spectrometry) age $^{206}\text{Pb}/^{238}\text{U} = 600.7 \pm 1.1$ Ma and $^{207}\text{Pb}/^{235}\text{U} = 602.2 \pm 1.0$ Ma (Jackson et al., 2004), PLESOVICE standard; known TIMS age $^{206}\text{Pb}/^{238}\text{U} = 337.13 \pm 0.37$ Ma and $^{207}\text{Pb}/^{235}\text{U} = 337.27 \pm 0.11$ Ma (Sláma et al., 2008). Data is then processed through Iolite (Hellstrom et al., 2008) for isotopic ages and U and Th counts.

3.2 Structural Mapping

The process of producing a structural map of Termination Valley involved field mapping geological features of the Burra and Umberatana rock group formations that make up the study area.

A3 aerial photos at the 1:5000 scale were primarily used for detailed field data plotting including but not limited to; strike and dip angle measurements, younging direction, fold axis tracing, fault tracing and lithological boundaries.

A3 aerial photos at the 1:14000 scale were also used for structural interpretation when not in a field setting, in order to locate and target complexities of interest within the field area, as well as a means of cross referencing location in the field with larger scale landscape features.

Measurements, photos, sample locations, descriptions and interpretations were all logged in a field notebook along with a GPS location corresponding to feature locality.

A Garmin Etrex 10 Personal GPS Unit set to AUS GEOD 1984 took GPS readings and was later integrated into ArcGIS 10.3.1 for more precise measurement plotting.

3.3 Cross sections

Cross sections are modelled on Corel Draw X7. Vertical cross-sections are modelled based on their calculated true formation thickness, using bedding angles taken in the field. Formation thicknesses on the hanging wall are taken from previously published estimations (Belperio, 1990; Mackay, 2011).

3.4 Sedimentology

Sedimentary logs were taken of the interpreted beginning of the Bolla Bollana Tillite Formation at a 1:200 scale. The traverse is taken by cutting perpendicular to strike of bedding and beginning at the interpreted boundary of the specific formation.

Using a tape measure and rope, structural readings, rock descriptions and unit surface lengths were taken with the intent to produce environmental interpretations of the sequence stratigraphy and hence the sedimentology at the time.

4 OBSERVATIONS AND RESULTS

4.1 Geological Map and Cross Sections

Figure 1 is a complete geological map of the Termination Valley area and its respective Neoproterozoic strata and interpreted structure. Five Neoproterozoic formations were encountered in the Termination Valley area, primarily consisting of Burra Group and Umberatana Group sedimentary formations.

A chronological sequence can be followed throughout the lithologies (see bottom left section of Figure 1 for sedimentary sequence) by traversing perpendicular to strike in the direction of younging (represented by stromatolite mounds and cross bedding indicators, Figure 2a, b, c). Lines A-A' and B-B' (Refer to Figure 1) are cross-section transects for the purpose of outlining major structural features in the area, an anticline and syncline pair.



GEOLOGY OF TERMINATION VALLEY
WITCHELINA SOUTH AUSTRALIA
NEOPROTEROZOIC GEOLOGY

THE UNIVERSITY
of ADELAIDE

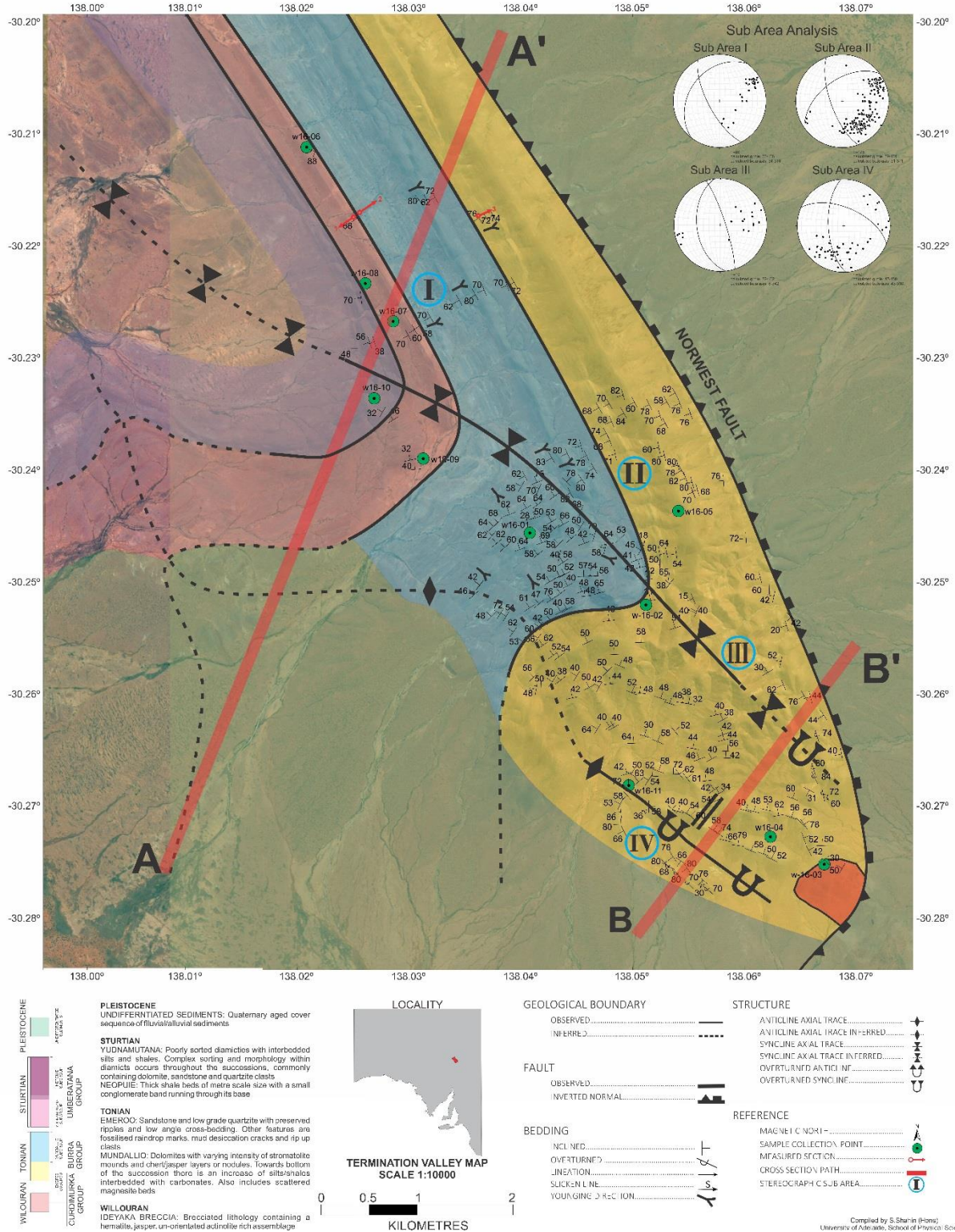


Figure 1: Geological Map of Termination Valley as mapped in field



Figure 2 Younging direction indicators. a/b) low angle cross beds in sandstones located in the Copley Quartzite Formation, c) Stromatolite mounds with 2 different cross sections, arrows imply younging direction, located in the Skillogalee Dolomite Formation

Cross-section A-A' (Figure 3) contains an anticline and syncline inclusive of all observed Umberatana and Burra Group formations, with an interpreted vertical extent of the anticline at approximately 3.71km based on lithology thicknesses, observed, and interpreted structure. Interpretation of lithologies on the eastern side of the Norwest Fault are based on information from publications and field observations (Belperio, 1990; Mackay, 2011). Curdimurka Group rocks underlie the Burra Group, although not observed in the field, this is a known stratigraphic relationship. Figure 3, shows the Termination Valley stratigraphy creating a 2-3km vertical extent above present day surface, with thrust strata along the Norwest Fault.

Cross-section B-B' (Figure 4) contains the anticline and syncline that outcrop through the Copley Quartzite Formation. The overturned trend of the anticline is apparent in the cross-section with the anticline tipping west. Similar to cross-section A-A' (Figure 3), over thrusting of underlying strata occurs along the Norwest Fault.

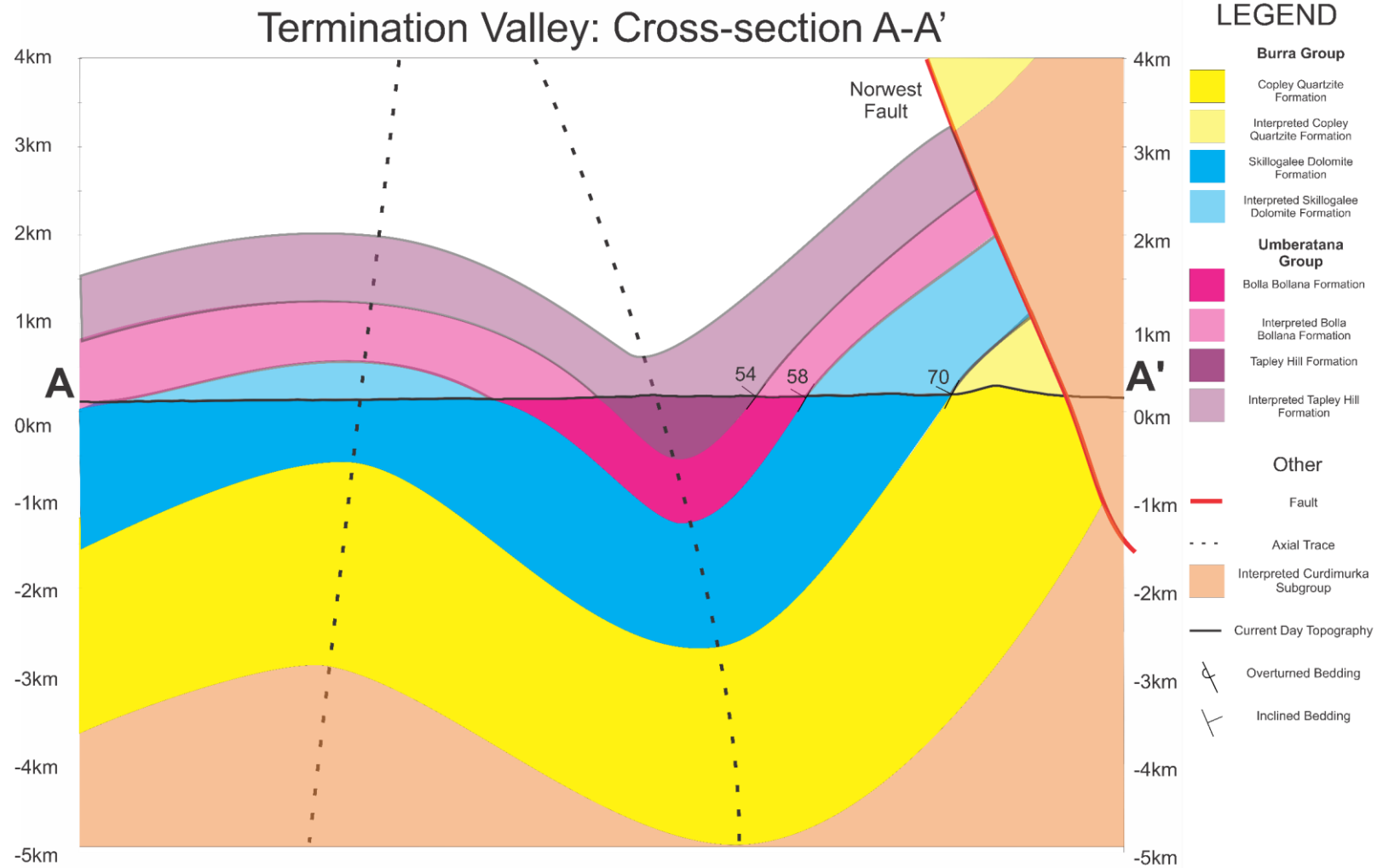


Figure 3: Vertical cross-section along transect A-A'
Note: Cross section reconstruction is modelled on interpreted geology prior to erosion.

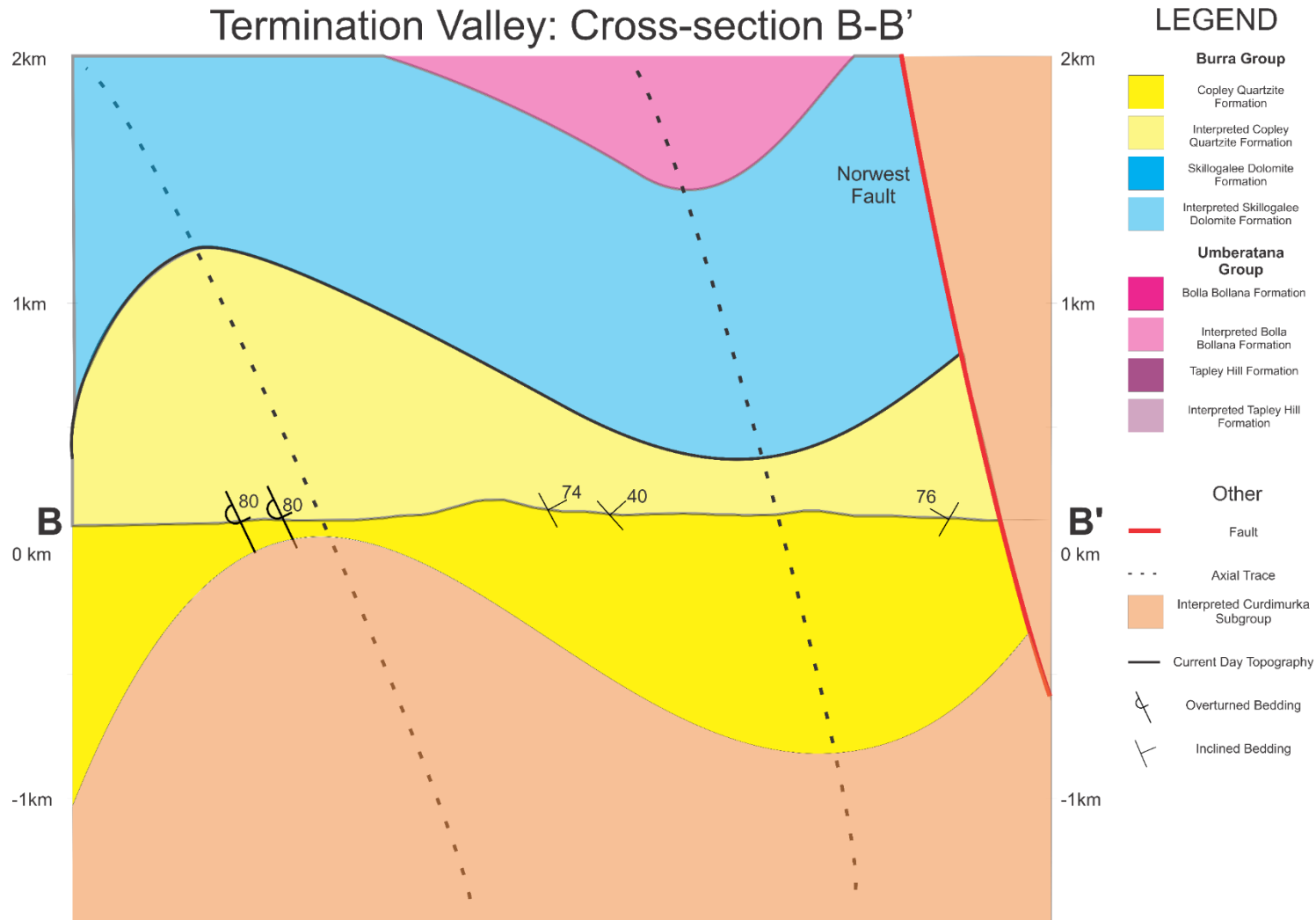


Figure 4: Vertical cross-section along transect B-B'
Note: Cross section reconstruction is modelled on interpreted geology prior to erosion.

4.2 Structural Facies Analysis

4.2.1 Regional structure and deformation

The Adelaide Rift Complex records deformation within its Paleo-Mesoproterozoic crystalline basement and Neoproterozoic sedimentary cover. General structural characterisation of the Northern Flinders Ranges and Willouran Ranges exists in the form of large open-scale folding of sedimentary rocks in fault controlled basins. Strain was focused along the major basement-rooted faults of the area, with minor variability and transfer to sedimentary decollements (Paul et al., 1999). This transfer is responsible for creating folding and variable deformation of overlying rocks.

4.2.2 Termination Valley D1

The Termination Valley area lies in the West Mount Domain on the foot wall of the Norwest Fault, and displays NW-SE trending folds, which is consistent with stereographic projections and mapping (Figure 5 and Figure 1).

D1 represents a deformation event linked to the Cambrian-Ordovician Delamerian Orogeny and has been interpreted by Murrell (1977) and Mackay (2011) as open-tight inclined folds, with varying plunge seen in Burra Group stratigraphy. Deformational events prior to the D1 in termination valley occur in the Willouran Ranges, but there is no evidence to suggest that the West Mount Domain, inclusive of Termination Valley, experienced any deformation relating to these event (Mackay, 2011). Delamerian style folding of the Neoproterozoic strata in the Termination Valley area was in the form of open to tight, upright to horizontally inclined concentric folds.

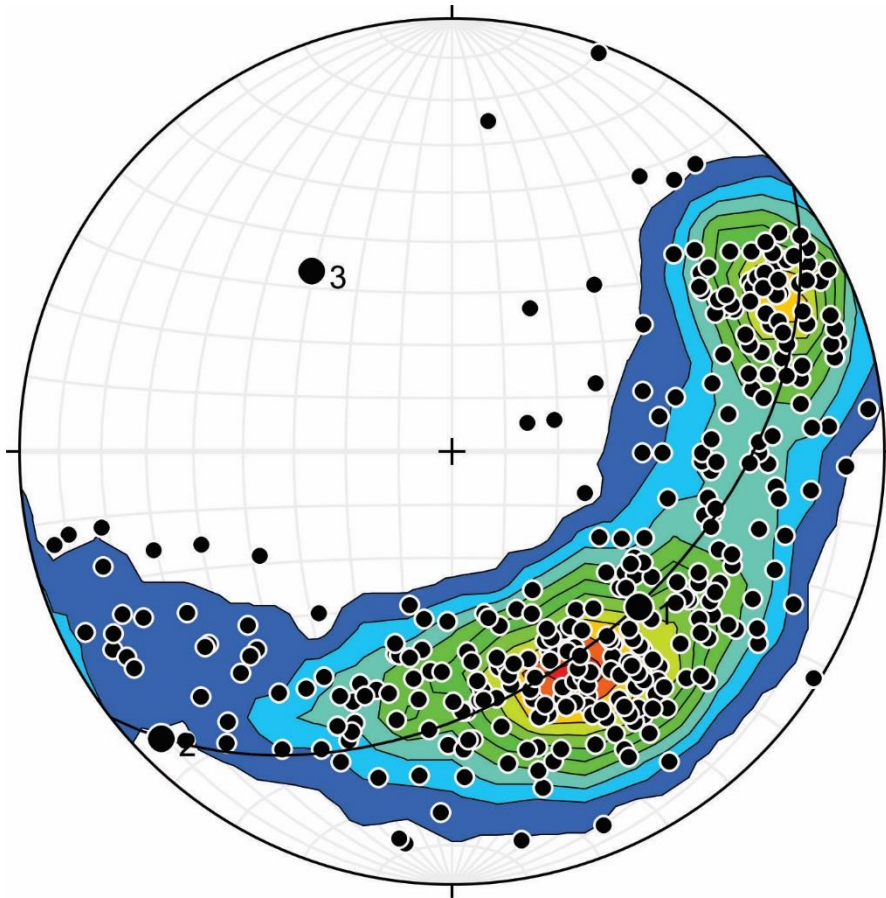


Figure 5: Stereonet of all structural data taken in field. Point “3” represents average pole to best fit plane of data. Red contour areas represent highest density of structural measurements and blue/white the least dense. Overall Structural trend of folds from total data represents a NW, moderately plunging folds.

4.2.3 Fold description

Folding is easily identifiable by the well bedded Copley Quartzite Formation rocks of Termination Valley, with the major synclines limbs easily seen from aerial photography from the respective NW-SE and NEE-SWW striking limbs. Parasitic folding is also preserved in the Burra Group, with a wavelength of ~15m, compared to the ~4km or greater, major conjugate fold outlined in Figure 1.

Cross section B-B' (Figure 4) shows NW plunging folds with an over turned anticline and conjugate, concentric, syncline outcropping in the Copley Quartzite Formation. Subarea analysis 4 is represented by a stereographic projection (Figure 7d). An inter limb angle of approximately 67° makes it a tight fold by classification (Fossen, 2010), with a hinge plunging towards 330° , which is consistent with interpreted fold structures of the North-Western Flinders zone (Mackay, 2011; Preiss, 1987; Rutland et al., 1981)

Development of the fold geometry in Termination Valley can be traced as the syncline plunges towards the NW. Beginning with an overturned limb component where it's observable, adjacently north of the Ideyaka Breccia (see Figure 1). The fold displays an inter limb angle of approximately 57° in Subarea 2, (open fold classification (Fossen, 2010)) and further north in Subarea 1 an angle of approximately 73° , showing a progressively tightening syncline. The presence of the anticline diminishes rapidly compared to the syncline, and its structure in cross-section A-A' Figure 3 is largely interpreted and lacks supporting data for characterisation in the north of Termination Valley.

4.3 Subarea Analysis

The Termination Valley area was split into 4 sub areas with the purpose of analysing the structural trends of folds in each locality. Selected subareas represent areas of spatial and structural difference. For all structural field data, refer to Appendix A: Structural Data. All subareas mentioned can be seen in Figure 6.

4.3.1 Subarea 1

Subarea 1 is the farthest north subarea with lithologies striking in a near parallel NW-SE trend. The NW-SE striking beds are represented by a large congregation of structural data in the top right quadrant of Figure 7a. Structural measurements close to the fold hinge of the syncline are represented by a small congregation of poles. An estimate of the axis of a cylindrical fold is found by taking the intersection of two great circles on a stereographic projection. The great circles must represent two distinct, opposing, limbs of a fold. This is known as a beta axis.

4.3.2 Subarea 2

Subarea 2 is a central subarea with a high density of data either side of the major synclinal fold of the region. The subarea structurally reflects both limbs of the syncline, and their gradual turning of bedding direction; the right limb facing the west, beds in the centre of the fold facing north, and the left limb pointing north east.

The stereonet in Figure 7b denotes this with 2 obvious data populations in the form of poles to bedding, but also a steady transition between the two, outlining the turning of the fold. Furthermore, 2 great circles representing the average planes of either limb of

the fold intersect with a calculated beta axis plunging at a direction of 51-311. This signifies a moderately plunging fold with a hinge pointing NW.

4.3.3 Subarea 3

Subarea 3 is located east of the syncline and bordering west of the Norwest Fault; a reactivated normal fault. Subarea 3 has 2 main population densities, the smaller of the two representing overturned beds, and the other normal bedding consistent with the west facing lithologies along the Norwest Fault. The intersection lineation of the two average population planes doesn't represent a fold hinge trend for this subarea as seen in Figure 7c.

4.3.4 Subarea 4

Subarea 4 lies entirely within the Copley Quartzite Formation where a major anticlinal feature outcrops. The structural data in Figure 7d shows two populations of poles to bedding representing both limbs of the fold, with a calculated beta axis direction of 43-330. The beta axis reflects a moderately plunging fold with a hinge pointing NW, consistent with the shape the fold takes in Figure 1, and consistent with the dip direction of readings around the limbs of the fold.

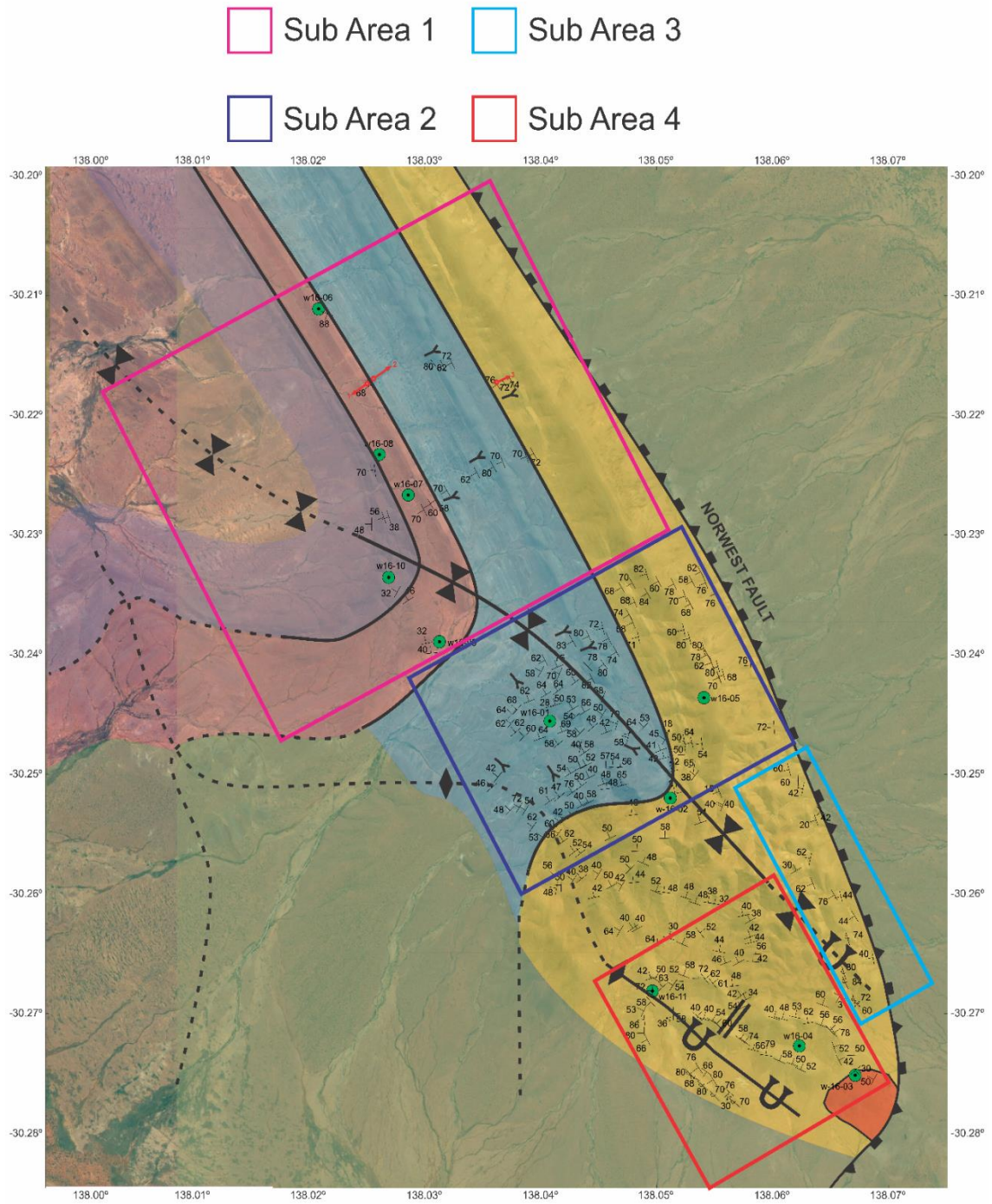


Figure 6: Geological map of Termination Valley with coloured boxes representing the groups of structural measurements that define each sub area analysis. Pink box=subarea 1, dark blue box=subarea 2, cyan box= subarea 3, red box=subarea 4.

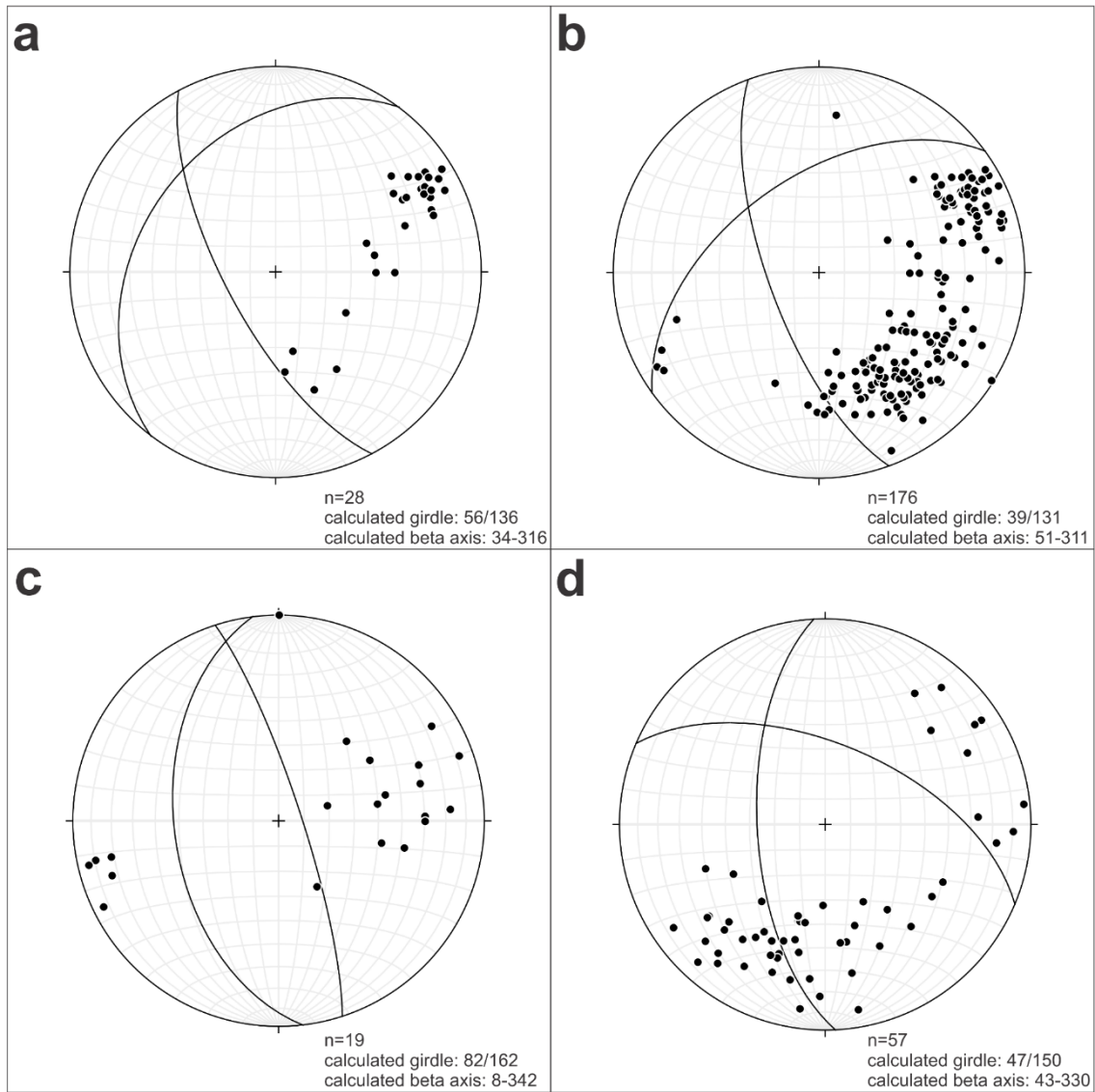


Figure 7: Stereographic projections for each subarea group, a) subarea 1, b) subarea 2, c) subarea 3, d) subarea 4

4.4 Sedimentology

The sedimentary formations in Termination Valley represent a sequence of sediments deposited on the footwall of the Norwest fault in the Willouran trough. The stratigraphy contains a depositional record extending from the Tonian (ca. 1000-720 Ma) to the Upper Cryogenian.

Table 1: Termination Valley formation key features

Formation	Key features
Ideyaka Breccia	Brecciated lithology containing a hematite, jasper, un-orientated actinolite rich assemblage. Interpreted as a diaporitic breccia predating deposition of the Burra Group
Copley Quartzite	Facies predominantly consist of sandstone and low grade quartzite with preserved ripples and low angle crossbedding. Other features are fossilised raindrop marks, mud desiccation cracks and rip up clasts.
Skillogalee Dolomite	Dolomites with varying intensity of stromatolite mounds and chert/jasper layers or nodules. Towards bottom of the succession there is an increase of silts/shales interbedded with carbonates. Occurrence of magnesite beds ranging from 1-20m ²
Bolla Bollana	Poorly sorted diamictites with interbedded silts and shales. Complex sorting and morphology within diamicts occurs throughout the successions, commonly containing dolomite, sandstone and quartzite clasts.
Tapley Hill	Largely made of a thick shale bed of metre scale size with a small conglomerate band running through its base.

4.4.1 Bolla Bollana Formation

The Sturtian aged Diamictite facies is a representative sedimentary sequence of multiple facies that characterise a fluvial-glacial deposit during deglaciation (see Figure 8 for representative facies images). It consists largely of matrix supported diamictites, deposited in an emergent to marine setting, with interbedded shales and conglomeritic packages of glacial sediments.

The use of the word tillite infers that the deposits are derived from the glacial till of the relative ice sheet, but the deposits of Termination Valley do not necessarily preserve strong evidence to suggest they are purely stratified till diamictites. For the purpose of this paper the specific deposits in Termination valley will be referred to as diamictites. The following sedimentary log (Figure 9) is a 208.16m section from the base of the Bolla Bollana Formation which is in contact with Burra Group rocks in the Termination Valley area.



Figure 8: Representative diamictite facies within the Bolla Bollana Tillite Formation

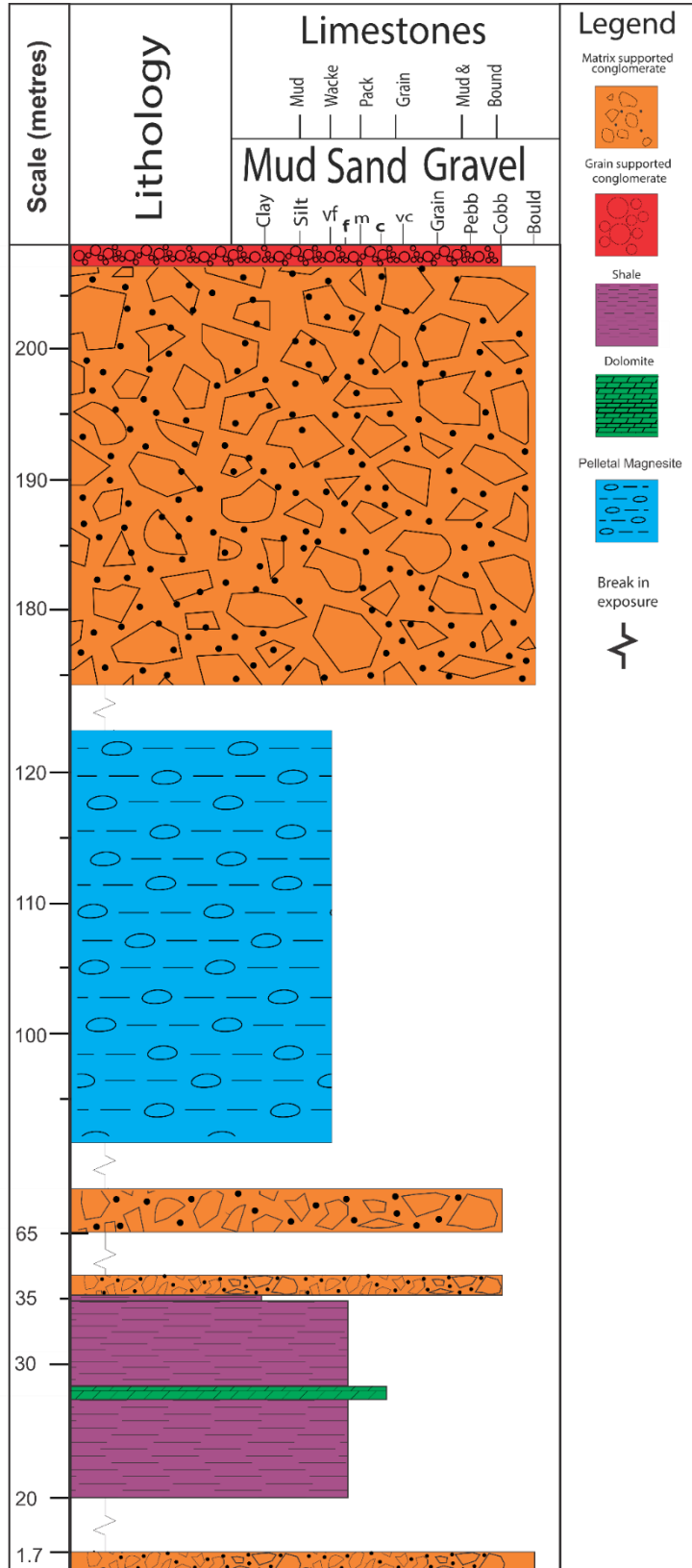


Figure 9: Sedimentary Log of Bolla Bollana Formation, taken from first Bolla Bollana Formation where in contact with the Burra Group rocks of Termination Valley.

Table 2: Lithofacies Summary of individual beds mapped in Sedimentary Log (Figure 9) of Bolla Bollana Tillite Formation

Lithofacies	Characteristics	Interpretations	Association	Formation
Matrix supported conglomerate	Poorly sorted Angular clasts of dolomite, pebbles and boulders of quartzite	Glacial melt drop off in shallow marine	Shallow water	Bolla Bollana
Grain supported conglomerate	Moderate-poor sorting of grain matrix consisting of siliciclastic grains sub-rounded.	Glacial melt drop off in shallow marine	Shallow water	Bolla Bollana
Shale	Grey-green with very weak to no cleavage.	Sub-wave base, anoxic environment. Glacial retreat.	Sub-wave base	Bolla Bollana
Dolomite	Yellow weathered surface, grey fresh dolomite	Shallow marine waters	Shallow water	Bolla Bollana
Pelletal Magnesite	Fine carbonate matrix with pelitic magnesite clasts and siliciclastic clasts suspended in matrix	Emergent to shallow marine	Shallow water	Bolla Bollana

4.4.1.1 Matrix Supported Conglomerate (MSC) Facies

Description:

The Matrix Supported Conglomerate (MSC) facies is comprised of a silt-clay matrix and includes clasts of; angular carbonates, pink-yellow in outcrop ranging from fine to pebble in size, well rounded quartzite and sandstone erratics, of boulder to pebble in size and sand-sized grains with sub-angular to rounded morphology. Matrix to clast ratio varies along strike, but generally does not exceed 20% clasts on the metre scale outcrop with the exception of sections containing large boulders. Lithologies and boulder erratics display crosscutting fracture sets, both along strike and perpendicular to it. Stratigraphic thicknesses can span metre to decimetre scale, commonly broken up by thin shale-silt sequences.

The MSC consists of siliciclastic or dolomitic clasts which could be interpreted to be older, lower lying stratigraphy of the Burra Group. Poor sorting of the facies and absence of drop stones or laminations in the facies places the depositional setting above the submarine shelf, and may characterise an intense deglaciation with till/glacier drop out.

4.4.1.2 Grain Supported Conglomerate (GSC) Facies

Description:

A siliciclastic grain supported matrix conglomerate with approximately 60% of the rock mass comprising of sub-rounded white clasts in contact with each other and space filled with a fine grained groundmass. Clasts are predominantly quartzite and sandstone, absent of any carbonate material with grain size ranging 1mm-2cm.

4.4.1.3 Shale Facies

Description:

Grey-green non-carbonaceous shales with intense fracturing. Quartz precipitation along fracture planes up to 1cm thick. Inside matrix of shale are minor (<1mm) and <1% ground mass of clasts suspended in shale matrix. Cleavage is weak or unpreserved. Shale outcrops in sets of fractured shale fingered members through metre thick beds.

4.4.1.4 Dolomite Facies

Description:

Yellow surfaced dolomite with grey-blue fresh surface. Outcropping in lenses across strike, with appearance similar to bedded dolomites in the older Burra Group, Skillogalee Dolomite Formation. Dolomite has thin (<1cm) bands of chert between bedding surfaces

4.4.1.5 Pelletal Magnesite Facies

Description:

A mudstone like facies with <10% grains of magnesite pellets and siliciclastic clasts. Clasts and pellets of angular-sub angular morphology, 1mm-5cm in size. The facies is weakly consolidated.

4.5 Geochronology

Zircons are a mineral belonging to the nesosilicate family. Zircons have become a widely used mineral for the purpose of extracting information on genesis of magmas, metamorphic events, and provenance of sedimentary rocks (Corfu et al., 2003).

Zircons are a suitable geochronometer based on the decay of U (and Th) to Pb, as zircons take up U and not Pb into their matrix during crystallisation. The decay of U to Pb can be tracked with the assumption that the zircon does not contain common lead at time of crystallisation.

U-Pb geochronology on detrital zircons using an LA-ICP-MS were conducted on samples W16-06, W16-07, W16-08, W16-09 from the Bolla Bollana Tillite Formation and W16-10 from the Tapley Hill Formation (Tindelpina Shale Member) of the Umberatana Group rocks in Termination Valley.

$^{206}\text{Pb}/^{238}\text{U}$ ages of detrital zircons ≤ 1500 Ma are used in any analysis presented here on including (probability density function plots (PDFPs), kernel density estimate plots (KDEPs), maximum age of deposition and multi-dimensional scaling (MDS)) (Spencer et al., 2016). Alternatively, detrital zircon ages > 1500 Ma are taken according to their $^{207}\text{Pb}/^{206}\text{Pb}$ age (Spencer et al., 2016). The parameters for age selection mentioned is based on a robust statistical analysis of LA-ICP-MS ablated zircons conducted by Spencer et al (2016). Zircons are targeted for ablation based on their cathodoluminescence signatures. Zircons with clear oscillatory zoning or xenocrystic cores were targeted specifically in an attempt to produce ages relative to magmatic crystallisation ages, with careful consideration into avoiding fractures or clear abnormalities in the crystals.

4.5.1 Sample W16-06

Belonging to the Bolla Bollana Tillite Formation, zircons in this sample are predominantly well rounded to sub rounded. They commonly display fine oscillatory zoning, zircons with high aspect ratios commonly display zoning patterns parallel to the long edge of the grain. Size varies from approximately 50-250 μm with the average size at approximately 160 μm . No evidence of metamorphic textures or rims exist, with many zircons experiencing fractures horizontal to long edge of grain.

118 detrital zircons were analysed with a total of 123 spots ablated over the whole sample. 69 spots returned data within 90-110% concordance.

4.5.2 Sample W16-07

Belonging to the Bolla Bollana Tillite Formation, zircons in this sample are mainly well rounded. Zircons displaying oscillatory zoning exhibit broad zoning patterns. In general, the whole sample contains zircons of low luminescence and an average zircon length of approximately 160 μm . Zircon lengths span 60-260 μm .

23 detrital zircons were analysed with a total of 31 spots ablated over the whole sample. 16 spots returned data within 90-110% concordance.

4.5.3 Sample W16-08

Belonging to the Bolla Bollana Tillite Formation, zircons from sample W16-08 display a broad range of morphologies with many zircons displaying euhedral shapes with very extinct edges.

Other zircons are sub-rounded but retain a euhedral shape and a proportion of the sample is very fractured and display no identifiable shape and are well rounded.

Luminescence is generally higher and many zircons display very fine oscillatory zoning.

The average zircon is approximately 170 μm with lengths ranging 60-300 μm .

83 detrital zircons were analysed with a total of 95 spots ablated over the whole sample.

61 spots returned data within 90-110% concordance.

4.5.4 Sample W16-09

Belonging to the Bolla Bollana Formation, this sample predominantly contains well rounded zircons. Zircons are generally broken horizontally through the middle with remaining well extinct edges. Zircons commonly display oscillatory zoning or no visible zoning at all. Zircon lengths range from approximately 70-350 μm with the average zircon length being approximately 200 μm . This sample on a whole contains large zircons in comparison to other samples.

73 detrital zircons were analysed with a total of 84 spots ablated over the whole sample.

62 spots returned data within 90-110% concordance.

4.5.5 Sample W16-10

Belonging to the Tapley Hill Formation, this sample predominantly contains broken fragments of zircons. The zircons in this sample generally have extinct fracture edges and well-rounded morphologies with very few extinct, euhedral shaped zircons.

Oscillatory zoning is commonly seen in many of the zircons. Zircon lengths range from approximately 50-440 μm with the average detrital zircon length being approximately 100 μm .

84 detrital zircons were analysed with a total of 100 spots ablated over the whole sample. 73 spots returned data within 90-110% concordance.

Figure 10 is a collation of representative concordant zircon grains imaged in CL from each sample. Table 3: Zircon descriptions, sample W16-06 Table 3a-e is a summary of key features of each zircon displayed in Figure 10.

Over the 5 individual samples, 433 zircon spots were analysed and 282 spots yielded data within 10% of concordance. All concordant data was plotted on a U-Pb Concordia diagram respective to each sample, seen in Figure 11a-e.

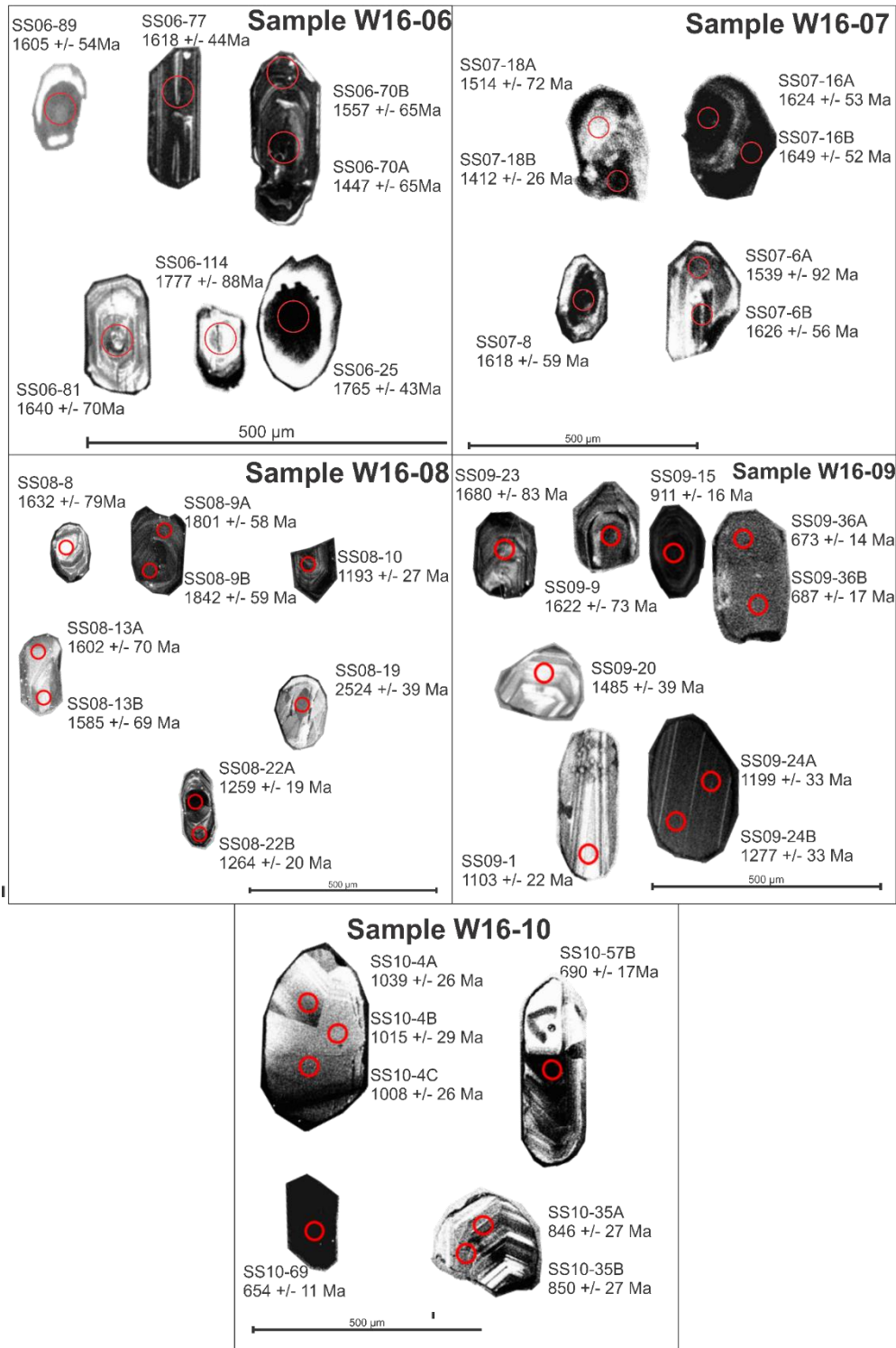


Figure 10: Representative detrital zircons from field samples (imaged under cathodoluminescence)

Table 3: Zircon descriptions, sample W16-06

W16-06							
spot number	Conc. %	Length μm	aspect ratio	morphology	visible core	luminescence	zoning
SS06-69	90.4	130	1.86	well rounded	yes	high	broad
SS06-77	95.9	200	2.86	extinct ends	no	low	fine parallel
SS06-70A/B	91.3&98.8	240	2.67	sub-rounded	yes	low	fine parallel
SS06-81	96.2	170	1.89	sub-rounded	yes	high	fine parallel
SS06-114	100.1	120	2	well rounded	yes	high	fine parallel
SS06-25	94.8	190	1.58	well rounded	yes	high	broad

Table 3b: Zircon descriptions, sample W16-07

W16-07							
spot number	Conc. %	Length μm	aspect ratio	morphology	visible core	luminescence	zoning
SS07-18A/B	104.2&91.9	250	1.67	well rounded	no	medium	fine
SS07-16A/B	94.2&94.9	260	1.24	well rounded	yes	low	fine-broad
SS07-8	100.6	160	1.75	well rounded	yes	medium	broad
SS07-6A/B	101.8&93	250	1.76	sub-rounded end (fractured in middle)	yes	high	fine-broad

Table 3c: Zircon descriptions, sample W16-08

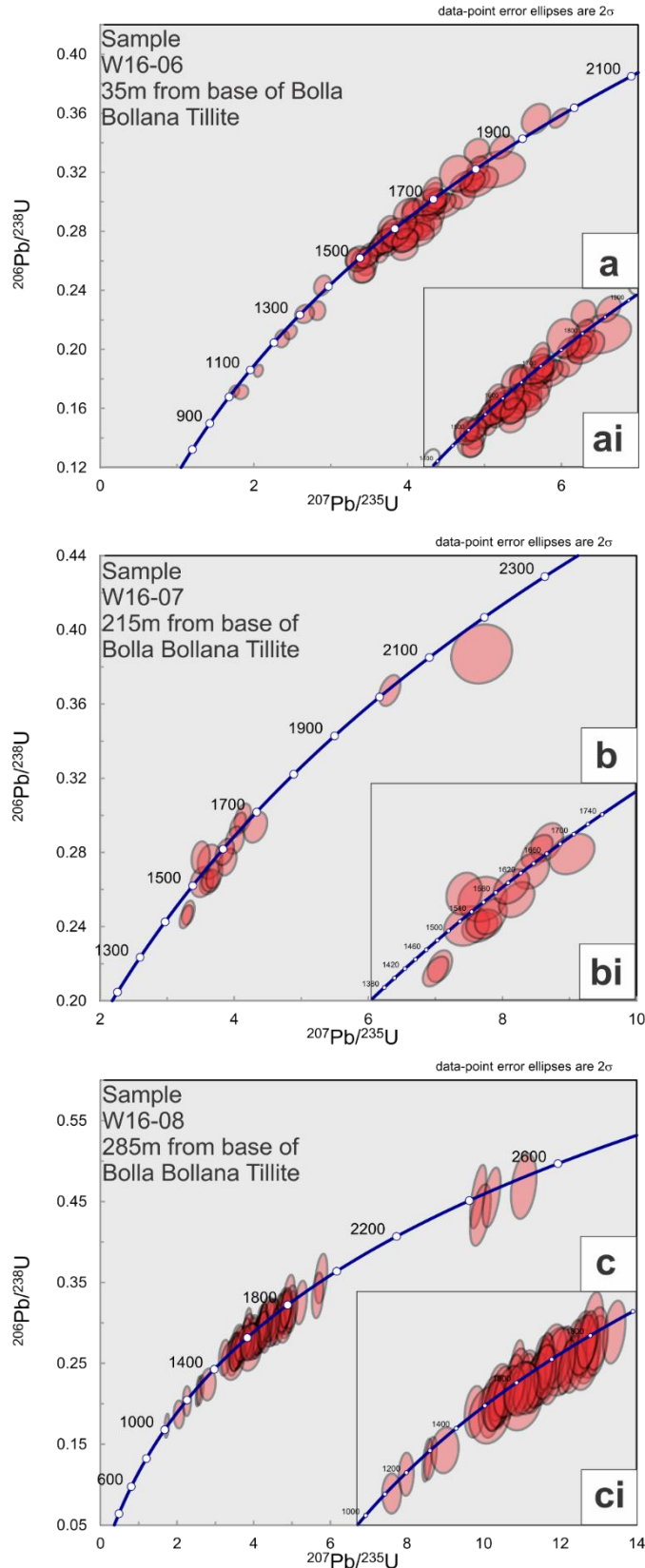
W16-08							
spot number	Conc. %	Length μm	aspect ratio	morphology	visible core	luminescence	zoning
SS08-8	98.7	160	1.6	well rounded	yes	high	fine
SS08-9A/B	97.9&93.8	230	1.64	well rounded	yes	low	fine
SS08-10	96.6	170	1.42	sharp extinct end (fractured in middle)	yes	low	fine
SS08-13A/B	101&100.4	220	1.83	well rounded	no	high	fine
SS08-19	98.2	200	1.54	well rounded	no	high	none
SS08-22A/B	95.8&92.8	220	2.75	sub-rounded	yes	medium	fine

Table 3d: Zircon descriptions, sample W16-09

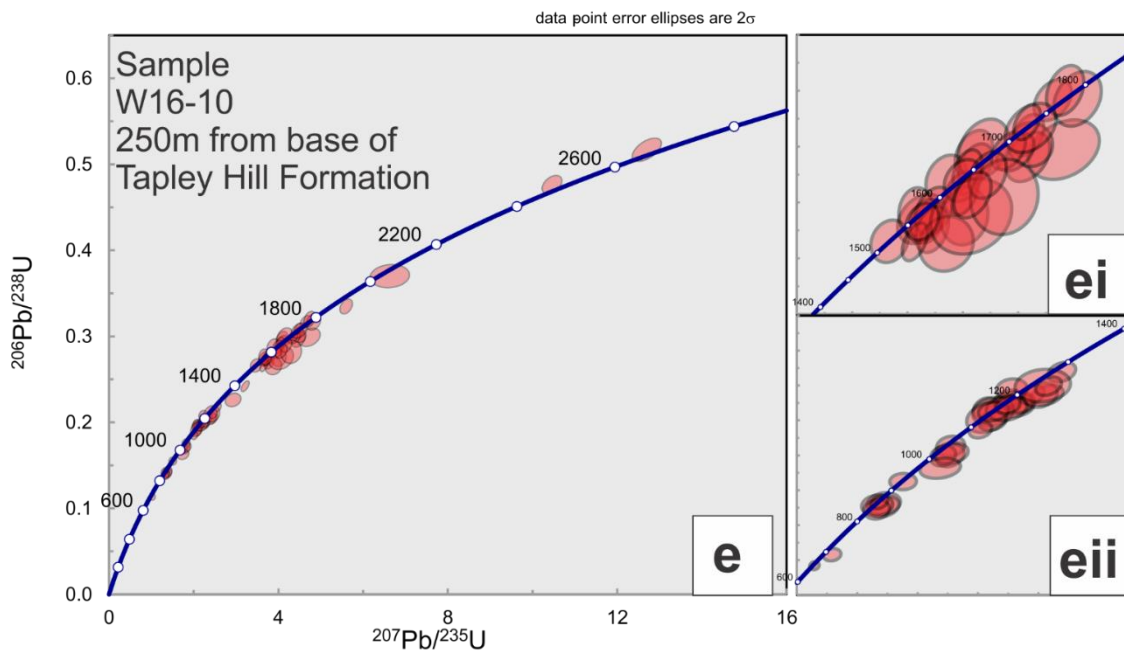
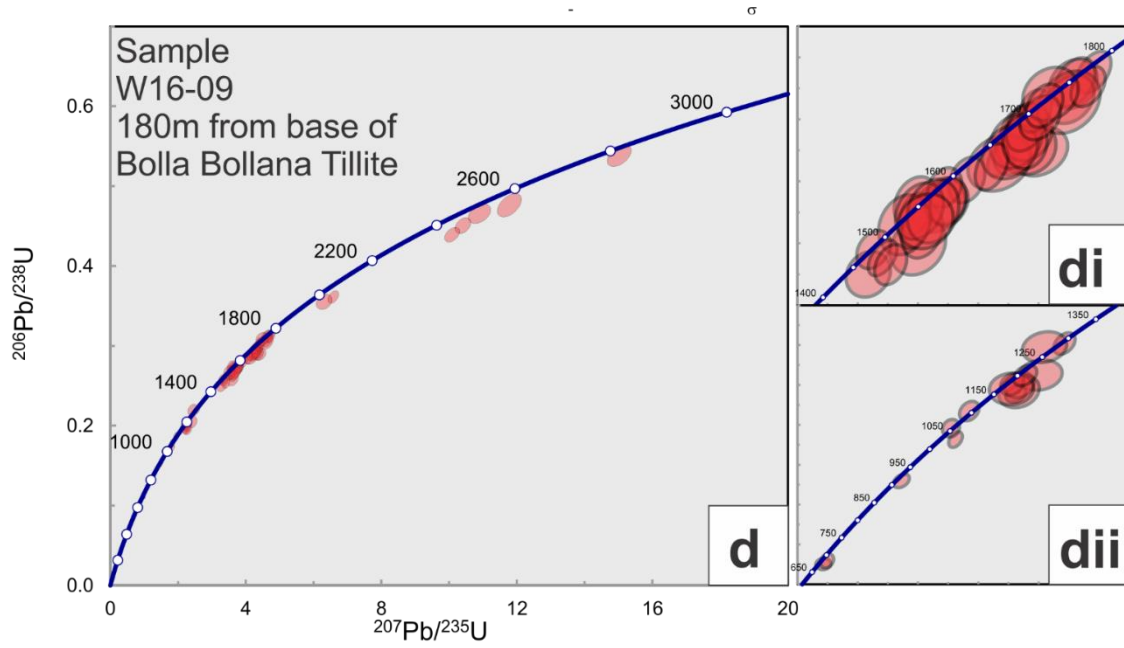
W16-09							
spot number	Conc. %	Length μm	aspect ratio	morphology	visible core	luminescence	zoning
SS09-23	96.5	200	1.43	well rounded	yes	medium	fine
SS09-9	95.4	210	1.5	sub-rounded	yes	medium	fine
SS09-15	94.9	210	1.75	well rounded	yes	low	fine
SS09-36A/B	100.9&96.1	300	1.67	well rounded	no	medium	none
SS09-20	91.4	180	1	well rounded	yes	high	fine
SS09-1	105.2	350	2.69	well rounded	no	high	fine parallel
SS09-24A/B	92.9&103.8	330	1.5	well rounded	no	low	fine parallel

Table 3e: Zircon descriptions, sample W16-10

W16-10							
spot number	Conc. %	Length μm	aspect ratio	morphology	visible core	luminescence	zoning
SS10-4A/B/C	100.8&94.4&95	420	1.91	well rounded	no	medium	broad
SS10-57	90.8	440	3.14	sub-rounded	yes	medium	fine
SS10-69	102.2	220	2	sub-rounded end and extinct end	no	low	none
SS10-35A/B	103.2&104.9	230	1	well rounded	no	high	fine



**Figure 11: U-Pb zircon age Concordia plots ($\pm 10\%$ concordance).
a) W16-06 concordia plot ai) W16-06 main age population b) W16-07 concordia plot bi) W16-07 main age population c) W16-08 concordia plot ci) W16-08 main age population**



d) W16-09 concordia plot di/ii) W16-09 main age population e) W16-10 concordia plot ei/ii) W16-10 main age population
For all U-Pb data refer to Appendix B: Geochronology

4.6 Age of deposition

It is common practice to constrain a maximum depositional age of a lithology by identifying a single detrital zircon of reliable concordance from within a sample.

Table 5 displays the single youngest concordant grain from each sample. As described by Dickinson et al (2009), the single youngest age of a zircon spot amongst all analysed zircon spots in a distinct lithology can provide an estimate on the maximum age of deposition for the rock group.

Table 4: Youngest Detrital Zircon summary

Sample	Maximum age of deposition (DZ)	Error 2 sigma	Concordance	Interpreted Formation
W16-06	1017	39	93	Bolla Bollana
W16-07	1412	52	92	Bolla Bollana
W16-08	1029	65	104	Bolla Bollana
W16-09	673	19	101	Bolla Bollana
W16-10	654	13	102	Tapley Hill

Spot SS10-69 from sample W16-10 yielded a single grain of age 654 ± 13 Ma and spot SS09-36B from sample W16-09 yielded an age of 673 ± 19 Ma, representing the 2 single youngest zircons for each interpreted formation.

4.7 Provenance

Multi-dimensional scaling (MDS) is a statistical technique used to compare data sets and model their similarity (Vermeesch, 2013; Vermeesch et al., 2016). As with any statistical technique, in this case a dimension reducing method, the models display an abstraction of the data for the purpose of visualising observations (U-Pb ages of detrital zircons).

Samples 6-9 lie within the interpreted Bolla Bollana Formation and show large similarities between one another, with the exception of sample 7, which alternatively bears a large similarity to the Curnamona province (Figure 12). The unique signature in sample W16-07 can be attributed to its small sample size (n=16) (refer to Appendix B: Geochronology). These similarities are to be expected, considering the samples lie within the same area and are deposited by what is likely the same mechanism. Sample W16-08 has a direct first order similarity with the Gawler Craton (see Figure 12), and sample W16-06 has a first order similarity with samples W16-08 and W16-09. The centre configuration for these three samples, which originate from the Bolla Bollana Formation, is likely attributed to their mixed signature. They likely contain remnant signatures from all three plotted provinces.

Sample W16-10 belongs to the interpreted Tapley Hill Formation, specifically the Tindelpina Shale member. This sample is shown to have a first order similarity to the Musgrave province, and a second order similarity to Sample W16-09 (see Figure 12).

Multi-Dimensional Analysis All Samples

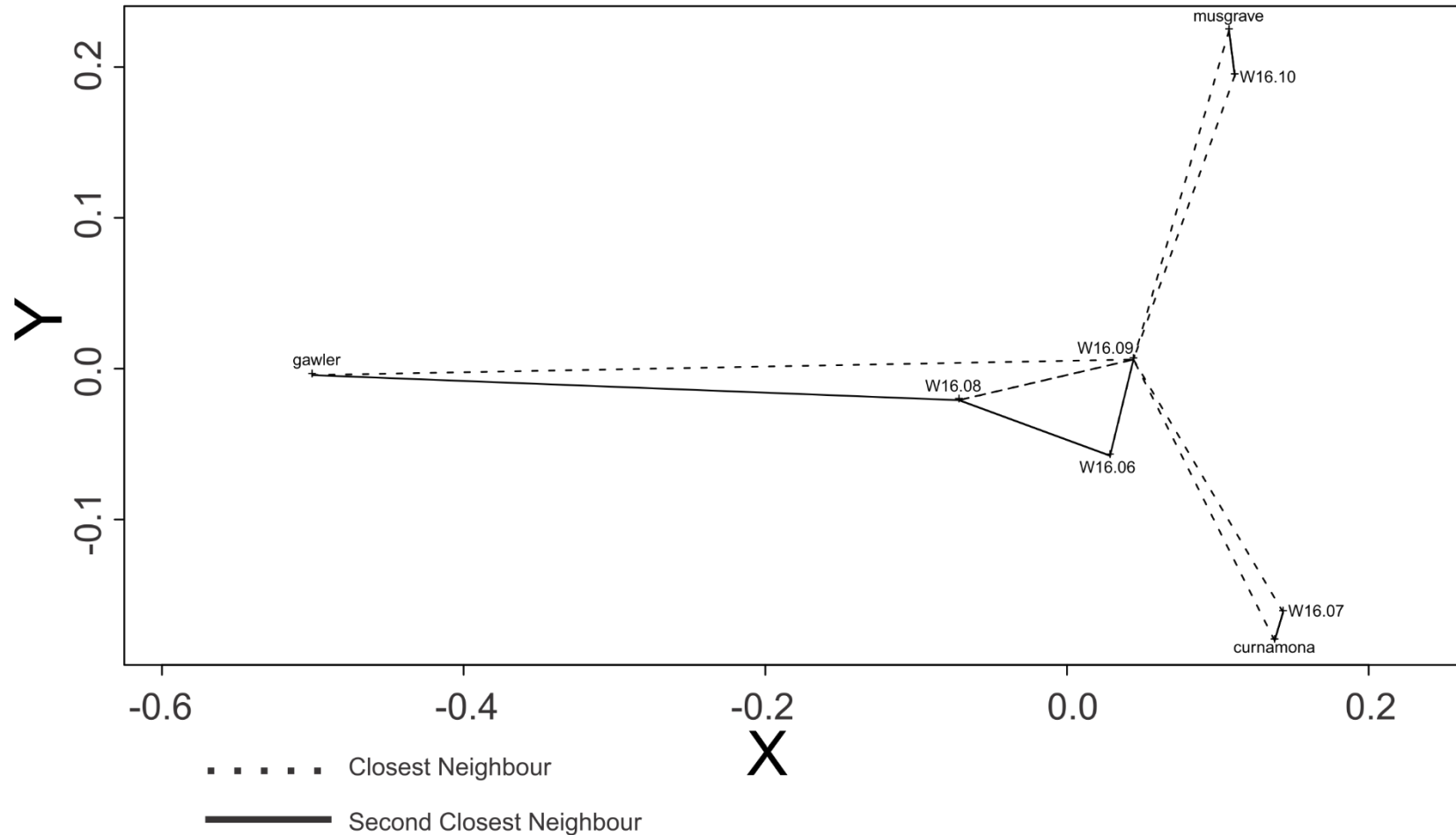


Figure 12: Multi-Dimensional Scaling plot of all field samples and 3 hypothesised proximal provinces (Gawler Craton, Musgrave Block and Curnamona Craton)

A kernel density estimation plot is a tool used to independently model a sample set. It is used for the purpose of making inferences on the population. The KDEPs (Kernel Density Estimate Plots) in Figure 13 represent the kernel density estimate function for each of the five samples and their respective concordant zircon ages.

Figure 14 is a series of probability density function plots (PDFPs). These plots model the zircon age estimates from each sample into a function that represents the distribution of the most probable zircon ages, and outlining minor and major age peaks that the sample data contains. Alongside the plot of all five field samples, is a plot of the signature given by the Elatina formation sourced from Rose et al. (2013), whilst the Dome Sandstone Formation of the Burra Group was sourced from Mackay (2011). Rose et al. (2013) have sampled from Mount Painter in the Far Northern Flinders Ranges and Mackay (2011) has sampled from the Willouran Ranges.

Table 5: Major and minor age peaks present in Kernel Density Estimate Plots

Sample	Major (Ma)	Minor (Ma)
W16-06	1680	1020, 1090, 1220
W16-07	1590	2050, 2280
W16-08	1650	2500
W16-09	1050, 1700	680, 1100, 2550
W16-10	1150, 1650	660, 850, 2500

Table 6: Major and minor age peaks present in Probability Density Function Plots

Sample	Major (Ma)	Minor (Ma)
W16-06	1570, 1600, 1680, 1760	1020, 1100, 1240, 1310, 1410, 1880, 1970
W16-07	1420, 1510, 1590, 1680	2010, 2110
W16-08	1495, 1600, 1700, 1800, 1850	1040, 1110, 1200, 1280, 1310, 2450, 2540
W16-09	1170, 1180, 1540, 1630, 1710, 1750	690, 910, 1020, 1070, 1110, 1300, 1990, 2350, 2400, 2490, 2780
W16-10	850, 1020, 1180, 1560, 1630, 1680	645, 700, 940, 990, 1280, 1320, 1400, 1780, 1860, 2030, 2510, 2690

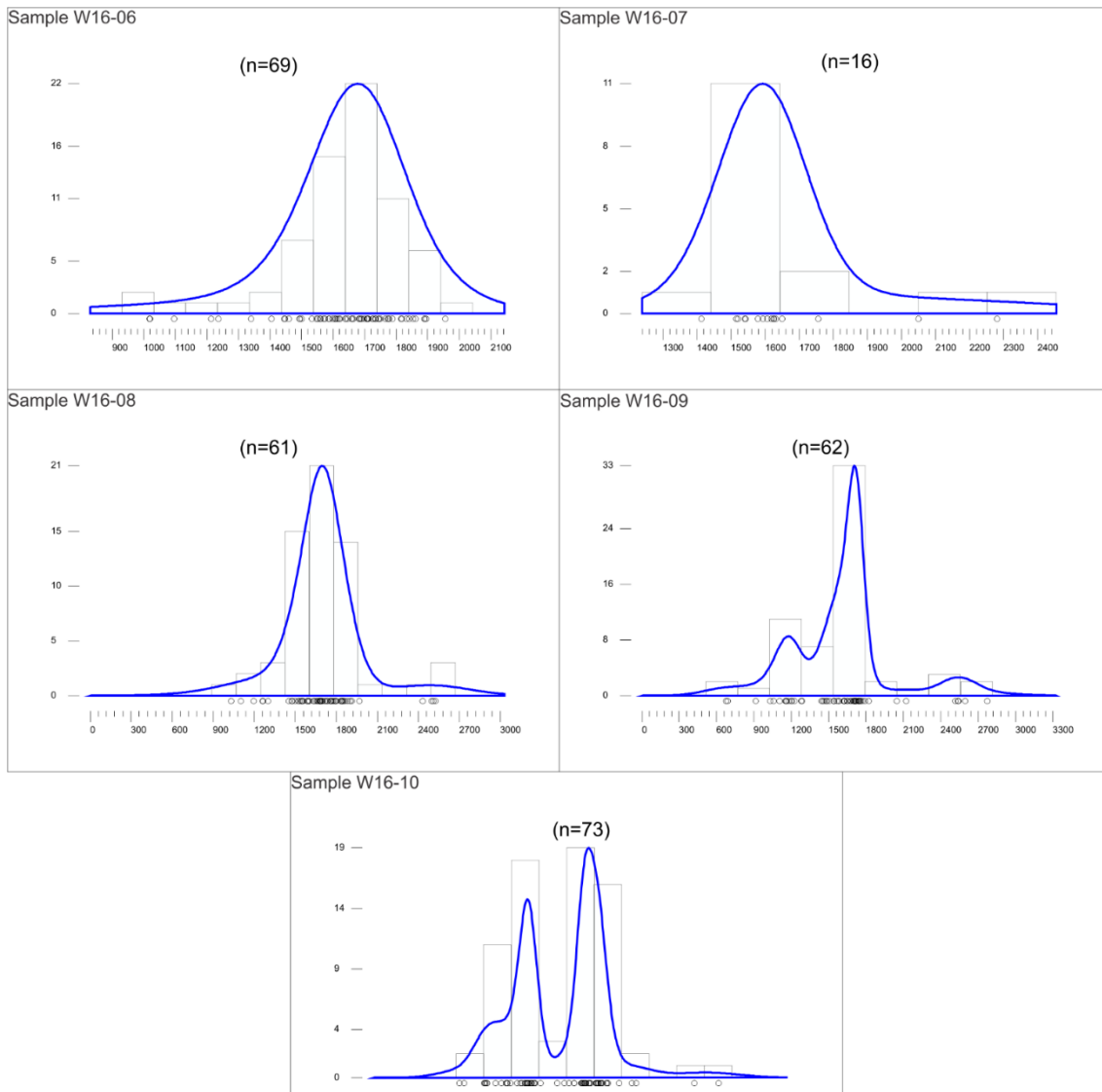


Figure 13: Kernel Density Estimate Plots of all samples

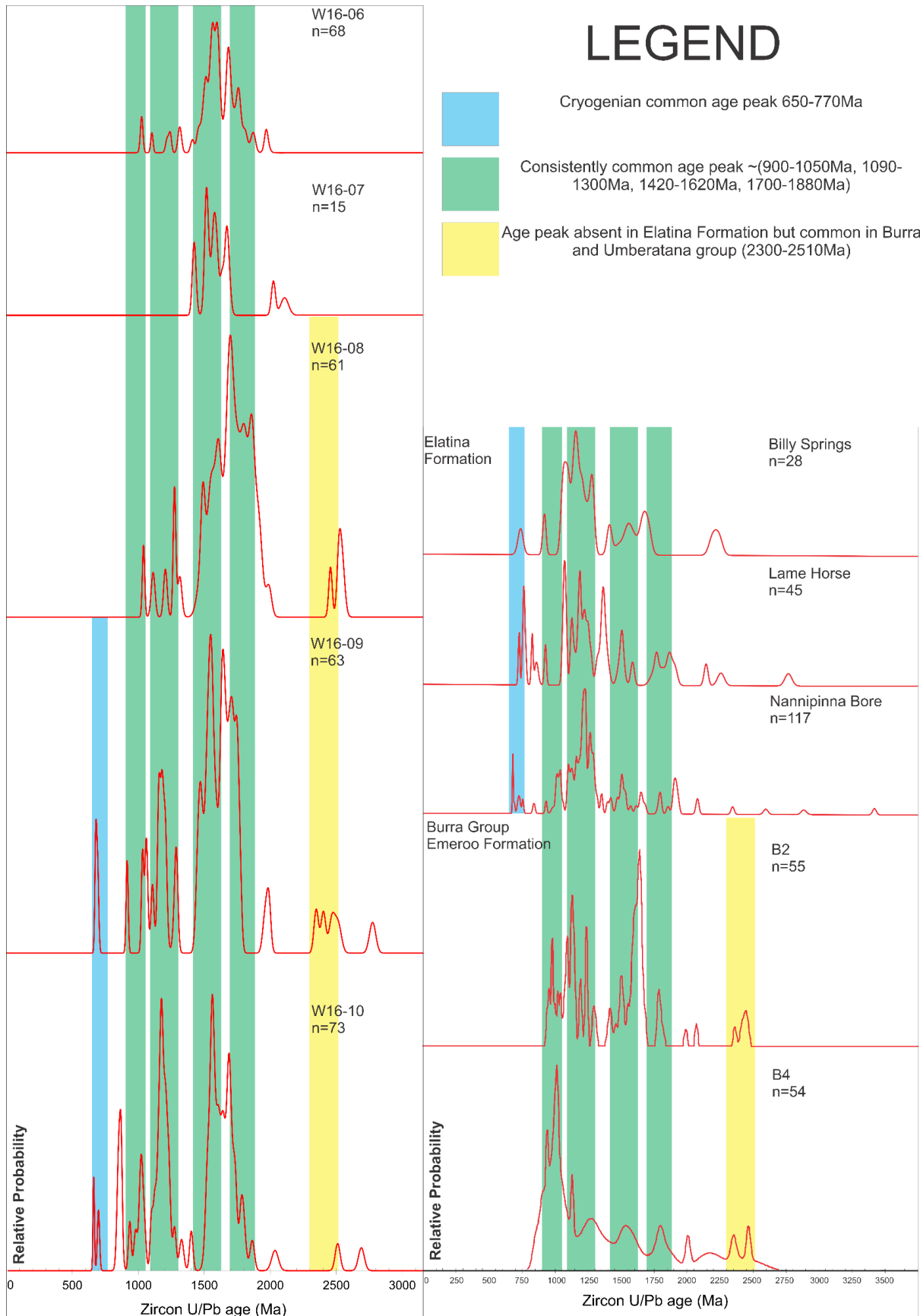


Figure 14: Probability density function plot for detrital zircon U-Pb ages. Plots on right represent samples taken from field area, Left represents Elatina Formation (post Umberatana deposit, modified from (Rose et al., 2013) and Burra Group (pre Umberatana deposit), modified from (Mackay, 2011)

5 DISCUSSION

5.1 Depositional Environment of the Lower Umberatana Group:

Characterising the depositional setting of the Lower Umberatana Group rocks in Termination Valley is done by compiling sedimentological features in the field, tectonic setting of the time and reference to facies modelling by Walker et al. (1992).

The Bolla Bollana Tillite Formation of Termination Valley displays a stratigraphic succession that implies a water lain mechanism for deposition. Along strike the diamictite facies exhibit variations in their matrix to clast ratio, with common lenticular bedding features. This can be interpreted as a fluvial glacial setting during deglaciation. As the glacier retreats during this Neoproterozoic deglaciation event, accumulated sediments and rocks drop out of the glacial ice, and are deposited in a complex fluvial system that features large water flow pathways and a glacially derived sediment source.

Diamictite facies are largely matrix supported, and could represent channel catchments where pebble to boulder size clasts drop out of the glacier and accumulate. With particular reference to Figure 9, matrix supported diamictites can often be succeeded or proceeded by finer grained sediments in a stratigraphic sequence, possibly representative of flood plains or banks in the system. Their relatively small stratigraphic thickness is implication for a local topography or sediment catchment style change, and not a marine transgressive sequence that would alternatively form larger bed thicknesses.

Overlying the Bolla Bollana Formation is the Tapley Hill Formation, a shale dominated unit. Termination Valley displays a conformably overlying shale formation above its glacial deposits, representative of marine transgression during deglaciation.

The diamictite-shale stratigraphic relationship is common throughout the Flinders Ranges. The glacial deposits of Termination Valley are similar to many cases reported and mapped throughout the Flinders Ranges (B. Forbes & Cooper, 1976; Link & Gostin, 1981; Preiss, 1987; Young & Gostin, 1989) in their stratigraphic sequences. Equivalent formations of Sturt Tillite in the Northern Flinders ranges have been characterised as glaciomarine deposits with significant sedimentary indicators such as drop stones (Daily, 1969; Link & Gostin, 1981), faceted and striated clasts (Link & Gostin, 1981; Parkin, 1969). Depositional environment and mechanisms cannot be assumed to be equivocal, and confident characterisation of the exact style of deposition would require a more in depth analysis of the sedimentology of the diamictites present in the study area.

5.2 Chronology of Cryogenian Glaciation

The single youngest detrital zircon of a sedimentary formation provides an estimate of the maximum age of deposition for said formation. With the single youngest zircon for the Bolla Bollana Formation, we know the oldest the deposit can be is its detrital zircon age of 673 ± 19 Ma. Kendall et al. (2006) has posited a Re-Os age constraint of 643.0 ± 2.4 Ma on the Tindelpina Shale Member of the Tapley Hill Formation in the Central Flinders Ranges. This formation is an equivalent of the Tapley Hill Formation in Termination Valley where sample W16-10 was taken (also from the Tindelpina Shale). Therefore it can be inferred that the demise of Sturtian glaciation was between 673 ± 19 Ma and 643 ± 2.4 Ma.

In North Western Canada a volcanic tuff interbedded with Sturtian glacial deposits was dated at 716.47 ± 0.24 Ma (Macdonald et al., 2010). Furthermore this zircon date is correlated with the Franklin Large Igneous Province (LIP).

The Franklin LIP is believed to have been emplaced when North Western Laurentia was within 10° of the equator, with significant research to support this (Evans, 2000; Palmer et al., 1983; Park, 1994). Although this is not directly correlative with Sturtian glaciation in the ARC, it suggests glaciation existed at low latitudes during this time. Research and supportive data for the commencement time of Sturtian glaciation in the ARC would estimate the duration of this glaciation period. Furthermore, it would link Rodinian derived continents, and their respective continental ice sheet cover, at tropical latitudes during the Neoproterozoic.

5.3 Detailed Analysis of Detrital Zircon signature and implications for provenance

Below is a detailed analysis of the major and minor peak spreads associated with the detrital zircon signatures derived from each sample and its respective kernel density estimate plot (KDEP) seen in Figure 13.

5.3.1 Major Peaks

Three major age peaks exist; 850 Ma, 1650 Ma and 1700-1780 Ma with associated shoulders. The 850 Ma peak that exists in sample W16-10 is made up of ages ranging 654-1100 Ma. The lower extent of this peak matches with ages corresponding to ages analysed in the O'Callaghans Supersuite from the Miles orogeny within the Paterson orogeny (Haines et al., 2013) or the Leeuwin Complex of Western Australia. The upper section can relate to ages analysed matching fine grained phyllitic metasandstones with an age of 870 ± 22 Ma (Haines et al., 2013), the Gairdner Dyke Swarm or the more proximal Wooltana Volcanics or Rook Tuff (Wingate et al., 1998).

1650 Ma is the largest and most common age peak, seen clearly in sample W16-06, W16-07 and W16-08 (refer to Figure 13). The age peak is made of a large range of ages spanning approximately 1530-1900 Ma and is associated with the 3 surrounding basins analysed in Figure 12. volcanics and granitic suits in the Gawler Craton within this age range include; Bosanquet formation, Myola volcanics, Tidnamurkuna volcanics, Wallaroo Group, McGregor volcanics, Middle Creek Granite, Tunkillia Suite, St Peter Suite Granites, Gawler Range volcanics and Hiltaba Suite Granites (Fanning, 2007; Hand et al., 2007). The Musgravian Gneiss from the Musgrave Block (1600-1550 Ma) are a similar aged source for the younger shoulder of the peak (Gray, 1978; Wade et al., 2008). The Curnamona Cratons Moolawatana suite rocks and box bore granite match ages from 1550-1583 Ma (Fraser & Neumann, 2010)

The Neoproterozoic was a time of intense glaciation and deglaciation with sedimentary records showing phases of continental ice sheet retreat and transgression. The detrital source analysis suggests zircon sources from igneous events extending to Western Australia and most notably the north lying Musgrave Block. This further suggesting an extensive land coverage of this Neoproterozoic glaciation period to the north and west

5.3.2 Minor Peaks

Three minor peaks are present; 670-690 Ma, 1050 Ma and 2450-2600 Ma. Firstly, a 670-690 Ma age peak, found in sample W16-09 is the youngest age peak found in all of the Bolla Bollana Formation samples. The ages can be related to ages seen in the O'Callaghans Supersuite, from the Miles orogen, within the Paterson orogeny (Haines et al., 2013), or the Leeuwin Complex of Western Australia.

The Leeuwin Complex formed in 3 distinct magmatic pulses spanning 1200-1050 Ma, 800-650 Ma and 580-500 Ma, with the 800-650 Ma event capable of accounting for this signature (Collins, 2003; Nelson, 1998).

Alternatively the Cotton Plateau Gabbros (ca 670 Ma) of East Antarctica fit this age peak but are less likely, considering sources suggest a north and west provenance (Goodge et al., 2002; Veevers et al., 2006).

A minor peak centres around 1050 Ma exists in sample W16-06 (Bolla Bollana Formation sample) that coincides with Musgrave province events such as the Warakurna Large Igneous Province (LIP) (1070-1080Ma) (Camacho et al., 2002; Sun et al., 1996). Alternatively it could correspond to a distal Leeuwin Complex magmatic event that was active 1200-1050 Ma (Collins, 2003; Nelson, 1998).

A common minor peak exists in all samples excluding W16-06 and is inclusive of samples in both the Bolla Bollana Formation and Tapley Hill Formation. The peak exists between 2450-2600 Ma and could be related to proximal sources such as the Curnamona Province metasediments or Gawler Cratons Sleaford Complex (Ashley et al., 1996; Cook et al., 1994; Hand et al., 2007; Raetz et al., 2002).

It may be interpreted that the detritus in the Bolla Bollana Formation can all be sourced from rocks found in north and west provenances. This suggests that ice sheets may have advanced from a broad north and westerly direction over the region now represented by the Willouran Ranges. This is consistent with the palaeogeography of Australia at ca. 700 Ma. According to Li et al. (2008), Australia lay at tropical northern latitudes at the time, which would mean that equatorially advancing ice sheets would be expected to come from the north. The overlying

Tapley Hill Formation has a distinctly different provenance signature (seen in Figure 12), that suggest a more restricted source from the Musgraves region to the NW (see Figure 15).

This suggests focussed sediment transport along the axis of the Willouran Trough from NW to SE, presumably down slope. Furthermore, the morphology of the zircons from the Tapley Hill Formation show extensive rounding and fracturing, suggesting a phase of re-working.

This can be attributed to the environmental setting of the deposit, a fluvial-alluvial system during an interglacial period. This suggests focussed sediment transport along the axis of the Willouran Trough from NW to SE, presumably down slope. Furthermore the morphology of the zircons from the Tapley Hill Formation show extensive rounding and fracturing, suggesting a phase of re-working. This can be attributed to the environmental setting of the deposit, a fluvial-alluvial system during an interglacial period.

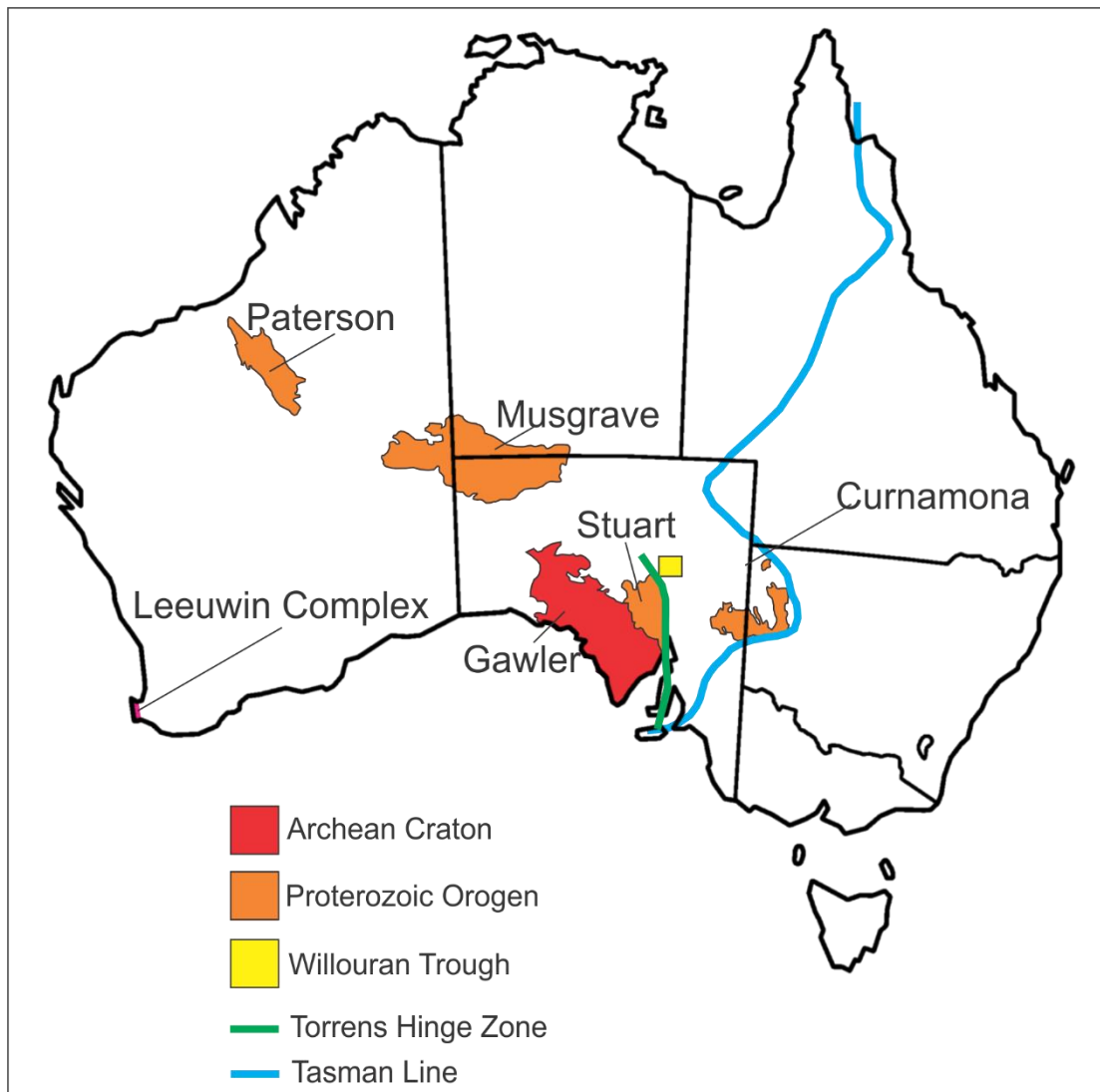


Figure 15: Cratonic Australia, with particular reference to possible provenance sources to the Willouran trough

6 CONCLUSION

The U-Pb ages of detrital zircons from this study help refine current Neoproterozoic chronology. Together with U-Pb ages presented in this paper, and previous Re-Os ages of the Tapley Hill Formation, a more refined and confident constraint on the demise of Sturtian glaciation in the Flinders Ranges can be made. A maximum age of deposition from the detrital study on the Bolla Bollana Formation has yielded an age of 673 ± 19 Ma, a previously un-dated formation. This age further confirms that the deposit is likely Sturtian in age, and belongs to the older of the two Neoproterozoic events.

Detrital zircon signatures from samples within Termination Valley suggest new insights into the sedimentary province of these glacially derived sediments. The distribution of zircon ages, with particular reference to the youngest minor age peaks of 700 and 654 Ma, indicate glacial sediments were derived from cratons of Western Australia. The zircon age signatures particularly highlight the significant input from the proximal Gawler Craton, Curnamona and most notably, the Musgraves. These prominent provenance signatures suggests focussed sediment transport along the axis of the Willouran Trough from the NW to SE and W to E, and are linked to similarly extending Sturtian ice sheets, prior to deglaciation and sedimentation.

Open to tight concentric folds, plunging in a NW direction are the main structural features in the Termination Valley area. These are consistent with D1 structures in equivalent Neoproterozoic strata of the Willouran Ranges, and are believed to be consistent with resultant deformation of the Cambrian-Ordovician Delamerian Orogeny. The orogeny is also believed to have caused final basin inversion and cessation of sedimentation in the area.

7 ACKNOWLEDGMENTS

Greatest of thanks to the staff and volunteers at the Nature Foundation SA for their sponsorship and interest in the project, with a particular thanks to the station managers (Brenton and Nannette Arnold, Kevin and Shirley Fahey, Phil Cole and Peter Collins) present during the field work for their company, assistance and warm hospitality .A special thank you to Prof. Alan Collins for his guidance and assistance throughout the duration of this project. Patrick James and Lange Powell for their company and enthusiasm during the field work and Patrick James' ongoing support and advice on matters regarding the geology of Termination Valley and the Witchelina area. Adelaide Microscopy staff, especially Aiofe Mcfadden and Benjamin Wade for their assistance in all aspects of detrital zircon imaging, ablation and data processing. A.Prof Vic Gostin for his invaluable advice and knowledge. Dr. Anthony Milnes for his words of encouragement and assistance in locating vital resources and publications. Dr. Juraj Farkas for constantly having his door open for discussion. Adrian Drabsch for his support and aid in map printing. Alex Ambrosi for his invaluable assistance in drafting. Matthew Drabsch for joining me on the rollercoaster that was our field work component and also everything associated with completing this thesis. And finally everyone that has continuously supported me in any way, shape or form throughout the year.

8 REFERENCES

- Allen, P. A., & Etienne, J. L. (2008). Sedimentary challenge to snowball Earth. *Nature Geoscience*, 1(12), 817-825.
- Ashley, P., Cook, N., & Fanning, C. (1996). Geochemistry and age of metamorphosed felsic igneous rocks with A-type affinities in the Willyama Supergroup, Olary Block, South Australia, and implications for mineral exploration. *Lithos*, 38(3), 167-184.
- Belousova, E., Reid, A., Schwarz, M., Griffin, W., & Fairclough, M. (2006). Crustal evolution of the Gawler Craton, South Australia: application of the TerraneChron technique to detrital zircon from modern stream sediments. *South Australia. Department of Primary Industries and Resources. Report Book*, 4, 192.
- Belperio, A. (1990). Palaeoenvironmental interpretations of the Late Proterozoic Skillogee Dolomite in the Willouran Ranges, South Australia. *The Evolution of a Late Precambrian–Early Palaeozoic Rift Complex: The Adelaide Geosyncline. Geol. Soc. Aust. Spec. Publ*, 16, 85-104.
- Brasier, M., McCarron, G., Tucker, R., Leather, J., Allen, P., & Shields, G. (2000). New U-Pb zircon dates for the Neoproterozoic Ghubrah glaciation and for the top of the Huqf Supergroup, Oman. *Geology*, 28(2), 175-178.
- Camacho, A., Hensen, B., & Armstrong, R. (2002). Isotopic test of a thermally driven intraplate orogenic model, Australia. *Geology*, 30(10), 887-890.
- Cardozo, N., & Allmendinger, R. W. (2013). Spherical projections with OSXStereonet. *Computers & Geosciences*, 51, 193-205.
- Collins, A. S. (2003). Structure and age of the northern Leeuwin Complex, Western Australia: constraints from field mapping and U–Pb isotopic analysis. *Australian Journal of Earth Sciences*, 50(4), 585-599.
- Cook, N., Fanning, C., & Ashley, P. (1994). *New geochronological results from the Willyama Supergroup, Olary Block, South Australia*. Paper presented at the Australian Research on Ore Genesis Symposium, Adelaide, Australian Mineral Foundation.
- Corfu, F., Hanchar, J. M., Hoskin, P. W., & Kinny, P. (2003). Atlas of zircon textures. *Reviews in mineralogy and geochemistry*, 53(1), 469-500.
- Daily, B., Forbes, B. G. (1969). Notes on the Proterozoic and cambrian, southern and central Flinders Ranges, South Australia. *Geological Excursions Handbook*, 3, 23-30.
- Evans, D. A. (2000). Stratigraphic, geochronological, and paleomagnetic constraints upon the Neoproterozoic climatic paradox. *American Journal of Science*, 300(5), 347-433.
- Fanning, C. M. a. (2007). *A geochronological framework for the Gawler Craton, South Australia*: Mineral Resources Group, Division of Minerals and Energy Resources, Primary Industries and Resources South Australia.
- Forbes. (1977). *The Boucaut Volcanics*: Department of Mines, South Australia.
- Forbes, B., & Cooper, R. (1976). The Pualco Tillite of the Olary region, South Australia. *Geological Survey of South Australia, Quarterly Notes*, 60, 2-5.
- Fossen, H. (2010). *Structural geology*. Cambridge New York: Cambridge University Press.
- Fraser, G. L., & Neumann, N. (2010). *New SHRIMP U-Pb Zircon Ages from the Gawler Craton and Curnamona Province, South Australia, 2008-2010*: Geoscience Australia.
- Goode, J. W., Myrow, P., Williams, I., & Bowring, S. A. (2002). Age and provenance of the Beardmore Group, Antarctica: constraints on Rodinia supercontinent breakup. *The Journal of Geology*, 110(4), 393-406.
- Gray, C. (1978). Geochronology of granulite-facies gneisses in the western Musgrave Block, Central Australia. *Journal of the Geological Society of Australia*, 25(7-8), 403-414.

- Haines, P., Wingate, M., & Kirkland, C. (2013). Detrital Zircon U–Pb Ages from the Paleozoic of the Canning and Officer Basins, Western Australia: Implications for Provenance and Interbasin Connections.
- Hand, M., Reid, A., & Jagodzinski, L. (2007). Tectonic framework and evolution of the Gawler craton, southern Australia. *Economic Geology*, 102(8), 1377-1395.
- Hearon, T. E., Rowan, M. G., Lawton, T. F., Hannah, P. T., & Giles, K. A. (2015). Geology and tectonics of Neoproterozoic salt diapirs and salt sheets in the eastern Willouran Ranges, South Australia. *Basin Research*, 27(2), 183-207.
- Hellstrom, J., Paton, C., Woodhead, J., & Hergt, J. (2008). Iolite: software for spatially resolved LA-(quad and MC) ICPMS analysis. *Mineralogical Association of Canada short course series*, 40, 343-348.
- Hoffman, P. F., Kaufman, A. J., Halverson, G. P., & Schrag, D. P. (1998). A Neoproterozoic snowball earth. *Science*, 281(5381), 1342-1346.
- Howard, K. (2006). Provenance of Palaeoproterozoic metasedimentary rocks in the eastern Gawler Craton, southern Australia: implications for reconstruction models of Proterozoic Australia. *University of Adelaide. BSc Hons thesis*.
- Jackson, S. E., Pearson, N. J., Griffin, W. L., & Belousova, E. A. (2004). The application of laser ablation-inductively coupled plasma-mass spectrometry to in situ U–Pb zircon geochronology. *Chemical Geology*, 211(1), 47-69.
- Kendall, B., Creaser, R. A., & Selby, D. (2006). Re-Os geochronology of postglacial black shales in Australia: Constraints on the timing of “Sturtian” glaciation. *Geology*, 34(9), 729-732.
- Kirschvink, J. L. (1992). Late Proterozoic low-latitude global glaciation: the snowball Earth.
- Le Heron, D. P., Cox, G., Trundle, A., & Collins, A. S. (2011). Two Cryogenian glacial successions compared: Aspects of the Sturt and Elatina sediment records of South Australia. *Precambrian Research*, 186(1), 147-168.
- Li, Z.-X., Li, X., Kinny, P., Wang, J., Zhang, S., & Zhou, H. (2003). Geochronology of Neoproterozoic syn-rift magmatism in the Yangtze Craton, South China and correlations with other continents: evidence for a mantle superplume that broke up Rodinia. *Precambrian Research*, 122(1), 85-109.
- Link, P. K., & Gostin, V. A. (1981). Facies and paleogeography of Sturtian glacial strata (late Precambrian), South Australia. *American Journal of Science*, 281(4), 353-374.
- Macdonald, F. A., Schmitz, M. D., Crowley, J. L., Roots, C. F., Jones, D. S., Maloof, A. C., . . . Schrag, D. P. (2010). Calibrating the cryogenian. *Science*, 327(5970), 1241-1243.
- Mackay, W. G. (2011). *Structure and sedimentology of the Curdimurka Subgroup, northern Adelaide Fold Belt, South Australia*. University of Tasmania.
- Mahan, K., Wernicke, B., & Jercinovic, M. (2010). Th–U–total Pb geochronology of authigenic monazite in the Adelaide rift complex, South Australia, and implications for the age of the type Sturtian and Marinoan glacial deposits. *Earth and Planetary Science Letters*, 289(1), 76-86.
- Nelson, D. (1998). Compilation of SHRIMP U-Pb zircon geochronology date, 1997. *Western Australia Geological Survey, Record*.
- Palmer, H., Baragar, W., Fortier, M., & Foster, J. (1983). Paleomagnetism of Late Proterozoic rocks, Victoria Island, Northwest Territories, Canada. *Canadian Journal of Earth Sciences*, 20(9), 1456-1469.
- Park, J. K. (1994). Palaeomagnetic constraints on the position of Laurentia from middle Neoproterozoic to Early Cambrian times. *Precambrian Research*, 69(1), 95-112.
- Parkin, L. W. (1969). *Handbook of South Australian Geology*: Geological Survey of South Australia.

- Paul, E., Flöttmann, T., & Sandiford, M. (1999). Structural geometry and controls on basement-involved deformation in the northern Flinders Ranges, Adelaide Fold Belt, South Australia. *An International Geoscience Journal of the Geological Society of Australia*, 46(3), 343-354. doi: 10.1046/j.1440-0952.1999.00711.x
- Powell, C. M., Preiss, W., Gatehouse, C., Krapez, B., & Li, Z. X. (1994). South Australian record of a Rodinian epicontinental basin and its mid-Neoproterozoic breakup (~ 700 Ma) to form the Palaeo-Pacific Ocean. *Tectonophysics*, 237(3), 113-140.
- Preiss, W. V. (1987). *The Adelaide Geosyncline : late Proterozoic stratigraphy, sedimentation, palaeontology and tectonics*. Adelaide: Govt. Printer, South Australia.
- Preiss, W. V. (2000). The Adelaide Geosyncline of South Australia and its significance in Neoproterozoic continental reconstruction. *Precambrian Research*, 100(1), 21-63. doi: 10.1016/S0301-9268(99)00068-6
- Raetz, M., Krabbendam, M., & Donaghy, A. (2002). Compilation of U–Pb zircon data from the Willyama Supergroup, Broken Hill region, Australia: evidence for three tectonostratigraphic successions and four magmatic events? *Australian Journal of Earth Sciences*, 49(6), 965-983.
- Rooney, A. D., Macdonald, F. A., Strauss, J. V., Dudás, F. Ö., Hallmann, C., & Selby, D. (2014). Re-Os geochronology and coupled Os-Sr isotope constraints on the Sturtian snowball Earth. *Proceedings of the National Academy of Sciences*, 111(1), 51-56.
- Rooney, A. D., Strauss, J. V., Brandon, A. D., & Macdonald, F. A. (2015). A Cryogenian chronology: Two long-lasting synchronous Neoproterozoic glaciations. *Geology*, 43(5), 459-462.
- Rose, C. V., Maloof, A. C., Schoene, B., Ewing, R. C., Linnemann, U., Hofmann, M., & Cottle, J. M. (2013). The end-Cryogenian glaciation of South Australia. *Geoscience Canada*, 40(4), 256-293.
- Rutland, R., Parker, A., Pitt, G., Preiss, W., & Murrell, B. (1981). The Precambrian of South Australia. *Developments in Precambrian Geology*, 2, 309-360.
- Sláma, J., Košler, J., Condon, D. J., Crowley, J. L., Gerdes, A., Hanchar, J. M., . . . Norberg, N. (2008). Plešovice zircon—a new natural reference material for U–Pb and Hf isotopic microanalysis. *Chemical Geology*, 249(1), 1-35.
- Spencer, C., Kirkland, C., & Taylor, R. (2016). Strategies towards statistically robust interpretations of in situ U–Pb zircon geochronology.
- Sprigg, R. (1952). Sedimentation in the Adelaide Geosyncline and the formation of the continental terrace. *Sir Douglas Mawson Anniversary Volume*, 153-159.
- Sun, S., Sheraton, J., Glikson, A., & Stewart, A. (1996). A major magmatic event during 1050–1080 Ma in central Australia, and an emplacement age for the Giles Complex. *AGSO Research Newsletter*, 24, 13-15.
- Veevers, J., Belousova, E., Saeed, A., Sircombe, K., Cooper, A., & Read, S. (2006). Pan-Gondwanaland detrital zircons from Australia analysed for Hf-isotopes and trace elements reflect an ice-covered Antarctic provenance of 700–500 Ma age, T DM of 2.0–1.0 Ga, and alkaline affinity. *Earth-Science Reviews*, 76(3), 135-174.
- Vermeesch, P. (2013). Multi-sample comparison of detrital age distributions. *Chemical Geology*, 341, 140-146.
- Vermeesch, P., Resentini, A., & Garzanti, E. (2016). An R package for statistical provenance analysis. *Sedimentary Geology*, 336, 14-25.
- Wade, B., Kelsey, D., Hand, M., & Barovich, K. (2008). The Musgrave Province: stitching north, west and south Australia. *Precambrian Research*, 166(1), 370-386.
- Walker, R. G., James, N. P., & Canada, G. A. o. (1992). *Facies Models: Response to Sea Level Change*: Geological Association of Canada.

- Wingate, M. T. D., Campbell, I. H., Compston, W., & Gibson, G. M. (1998). Ion microprobe U–Pb ages for Neoproterozoic basaltic magmatism in south-central Australia and implications for the breakup of Rodinia. *Precambrian Research*, 87(3–4), 135-159. doi: [http://dx.doi.org/10.1016/S0301-9268\(97\)00072-7](http://dx.doi.org/10.1016/S0301-9268(97)00072-7)
- Young, G. M., & Gostin, V. A. (1989). An exceptionally thick upper Proterozoic (Sturtian) glacial succession in the Mount Painter area, South Australia. *Geological Society of America Bulletin*, 101(6), 834-845.
- Zhang, S., Jiang, G., Zhang, J., Song, B., Kennedy, M. J., & Christie-Blick, N. (2005). U-Pb sensitive high-resolution ion microprobe ages from the Doushantuo Formation in south China: Constraints on late Neoproterozoic glaciations. *Geology*, 33(6), 473-476.

9.1 APPENDIX A: STRUCTURAL DATA

Table 7: Structural bedding readings and locations

id no.	latitude	longitude	altitude	dip	dip direction
31	-30.242112	138.035354	205.543869	63	341
35	-30.243632	138.037945	228.55983	68	325
38	-30.245237	138.039126	233.306335	69	345
39	-30.245729	138.040439	234.332855	52	283
40	-30.246339	138.041141	240.559509	40	326
45	-30.249268	138.045149	358.765625	65	345
46	-30.250971	138.049475	326.891937	60	344
48	-30.249932	138.050562	290.019714	31	349
49	-30.24992	138.050566	291.175293	44	328
50	-30.24904	138.051016	278.101898	38	356
53	-30.246953	138.051414	262.721954	34	345
54	-30.246953	138.051416	262.117188	36	297
55	-30.24649	138.051325	258.187561	50	284
56	-30.246593	138.049853	254.157822	41	309
59	-30.244079	138.047252	239.696945	53	316
68	-30.275306	138.068917	177.056107	32	91
69	-30.275305	138.068916	177.042725	30	140
75	-30.273073	138.069361	182.350235	50	358
79	-30.268005	138.069027	170.267822	73	244
80	-30.267953	138.067342	210.625671	31	208
81	-30.268736	138.066323	192.497498	60	20
82	-30.270345	138.06569	212.144638	80	350
83	-30.26993	138.065664	228.672592	80	350
85	-30.272698	138.063061	192.437424	64	24
87	-30.27255	138.063379		70	219
90	-30.208105	138.012674	238.126709	88	200
96	-30.242791	138.041169	286.697266	54	331
97	-30.242255	138.041486	268.976898	55	290
98	-30.240599	138.042301	220.432465	80	7
99	-30.239904	138.041407	220.39241	82	242
100	-30.239552	138.041192	216.014862	61	59
101	-30.239207	138.041654	243.265503	54	45
102	-30.238875	138.04223	270.235321	80	60
104	-30.238699	138.042618	257.316895	60	234
105	-30.23825	138.043456	230.555573	74	64
106	-30.237612	138.043948	226.527679	60	240
191	-30.23623	138.046344	248.231354	71	258
192	-30.23433	138.045275	264.501831	74	240
193	-30.235462	138.042611	226.175079	72	256
194	-30.235998	138.041051	216.548584	64	252

195	-30.23631	138.040039	222.428101	70	62
197	-30.237017	138.039548	220.436539	83	245
198	-30.239487	138.04082	216.440475	78	62
199	-30.240139	138.040207	224.423965	64	324
200	-30.240637	138.039894	230.060577	60	302
204	-30.241387	138.042865	223.387802	68	290
206	-30.241836	138.043021	241.601883	59	292
207	-30.242107	138.042989	246.501251	66	296
208	-30.242968	138.042888	237.001862	88	302
209	-30.243664	138.042509	239.103577	58	304
210	-30.244084	138.041996	253.09317	48	320
211	-30.244617	138.040587	244.68042	58	316
212	-30.245191	138.039256	229.442566	58	326
213	-30.245613	138.03834	233.576324	58	322
214	-30.245711	138.037306	239.740417	32	338
235	-30.245187	138.036527	259.706238	64	342
236	-30.245193	138.036484	259.513092	52	316
279	-30.244934	138.034739	237.699814	60	318
280	-30.244664	138.034201	229.376465	64	326
281	-30.244306	138.03373	208.628174	62	320
284	-30.243776	138.033334	211.65329	58	310
285	-30.243389	138.033808	212.779434	62	324
286	-30.242912	138.033477	206.990524	64	314
287	-30.242559	138.033962	205.519669	68	312
288	-30.241902	138.035395	208.314102	62	340
289	-30.241563	138.036006	211.279572	62	318
290	-30.241247	138.037145	217.168198	64	330
291	-30.240473	138.037649	212.036041	68	330
292	-30.239981	138.038212	215.848221	70	330
293	-30.23938	138.0383	217.650909	75	294
294	-30.239068	138.038506	217.919403	64	334
295	-30.2389	138.03836	221.05748	82	338
296	-30.238324	138.03647	221.857224	62	243
297	-30.239178	138.036422	213.753387	58	300
305	-30.23196	138.044475	254.779327	68	240
306	-30.231841	138.045052	267.276276	70	240
307	-30.231339	138.045659	286.87561	58	237
309	-30.230717	138.047185	386.743134	82	254
310	-30.23141	138.048338	397.664978	60	242
311	-30.231634	138.049969	374.133972	30	244
312	-30.231385	138.050357	365.971008	78	58
313	-30.230928	138.049772	348.659851	62	72
315	-30.232033	138.050859	350.713409	58	242
316	-30.232654	138.051182	346.466492	70	252

317	-30.233388	138.05169	358.711365	68	241
318	-30.235603	138.05108	391.075317	60	258
322	-30.236355	138.05167	389.952942	80	256
323	-30.237253	138.053125	364.221375	80	256
325	-30.237813	138.053453	382.127808	78	240
328	-30.238494	138.053951	372.348572	62	250
329	-30.238849	138.054658	361.465057	80	254
330	-30.239812	138.054746	346.891449	70	250
332	-30.239588	138.055251	312.344696	68	254
333	-30.238673	138.058134	244.034317	76	266
341	-30.238237	138.060035	204.650391	82	252
347	-30.233358	138.063109	174.131439	86	244
437	-30.23168	138.058193	186.315857	62	234
438	-30.232435	138.054462	224.968536	76	250
439	-30.231621	138.053666	225.304916	66	186
442	-30.231507	138.053311	231.78981	76	248
443	-30.23149	138.052636	241.936783	70	252
444	-30.2314	138.051872	277.86087	62	242
445	-30.232461	138.047185	342.346039	84	240
446	-30.233204	138.0459	307.223846	68	248
447	-30.235001	138.045678	247.26178	68	246
448	-30.236409	138.04315	226.108917	78	244
449	-30.236201	138.041083	224.690155	68	246
450	-30.236274	138.040225	233.666275	80	240
451	-30.236658	138.039371	219.037918	72	240
468	-30.242427	138.039064	235.343445	60	330
469	-30.242532	138.039909	256.43866	50	330
471	-30.241934	138.039356	246.043549	42	334
472	-30.243174	138.040156	282.885468	66	320
473	-30.244078	138.041932	249.075027	40	334
474	-30.24344	138.0427	243.012924	58	320
475	-30.243213	138.043064	249.164764	50	274
476	-30.243129	138.043344	252.139694	58	296
477	-30.244179	138.043406	258.829773	42	340
478	-30.244679	138.045239	249.931793	62	272
479	-30.244983	138.04542	259.015839	62	284
484	-30.247708	138.045042	272.858246	56	356
485	-30.247781	138.044223	281.416473	54	5
486	-30.247848	138.043513	273.286621	57	1
487	-30.248207	138.042595	264.814636	56	332
488	-30.247492	138.041313	258.439117	58	332
489	-30.247691	138.040783	254.483444	52	336
490	-30.247773	138.039891	248.272873	54	342
491	-30.249223	138.040825	264.532562	50	322

492	-30.249814	138.039852	281.79303	76	325
493	-30.2502	138.038482	249.538208	47	320
494	-30.250603	138.037501	236.46019	61	326
495	-30.251332	138.034799	231.980225	54	302
496	-30.251098	138.034153	226.971039	72	302
498	-30.252807	138.035596	221.438721	62	306
499	-30.25347	138.036138	245.147339	54	298
500	-30.253678	138.036587	263.356873	53	302
501	-30.253734	138.037735	278.842102	66	302
502	-30.25411	138.038935	298.441864	62	326
503	-30.255022	138.04007	359.12854	52	324
504	-30.255145	138.040697	373.646576	54	323
505	-30.25385	138.043856	409.438538	50	335
506	-30.255079	138.046831	427.328979	50	357
507	-30.256294	138.047442	413.735809	48	22
508	-30.256499	138.045888	381.386261	50	316
509	-30.258056	138.043986	358.271027	50	332
511	-30.259102	138.042271	365.655853	42	348
512	-30.256929	138.042458	267.813995	40	302
513	-30.257387	138.040795	256.938416	38	322
514	-30.257475	138.039819	250.218246	40	305
515	-30.257908	138.038347	242.360382	48	272
516	-30.25817	138.037906	229.171356	50	280
517	-30.257398	138.038063	240.096817	66	312
518	-30.257051	138.037899	240.390839	56	316
519	-30.253978	138.038052	273.620789	56	320
520	-30.253173	138.038266	261.364868	60	306
521	-30.252604	138.038248	242.043655	60	326
523	-30.252333	138.038404	233.683746	42	304
524	-30.252198	138.038895	248.700943	50	310
525	-30.251774	138.039797	269.470764	40	318
526	-30.251593	138.040416	280.210907	50	358
527	-30.250969	138.0409	312.825684	40	330
528	-30.250748	138.041582	336.10376	58	330
529	-30.250027	138.040245	297.688385	40	328
530	-30.24803	138.0397	237.571655	50	330
532	-30.24528	138.03908	229.882141	52	330
533	-30.244561	138.038896	217.837341	54	340
534	-30.243929	138.03847	212.882278	60	346
536	-30.243205	138.037878	204.425293	40	334
538	-30.226304	138.018489	183.149658	40	270
539	-30.226308	138.018597	181.274933	48	270
542	-30.2259	138.019168	194.178101	40	260
545	-30.225808	138.019486	202.578461	56	250

547	-30.225719	138.020186	199.11377	38	252
556	-30.225169	138.023817	189.262192	70	242
558	-30.224644	138.024492	199.871353	60	240
559	-30.224418	138.024822	193.745956	58	236
561	-30.223471	138.026202	200.236938	70	240
566	-30.22188	138.02932	223.148743	62	240
567	-30.221753	138.029774	211.705017	76	236
571	-30.221374	138.031086	204.814377	80	240
572	-30.221227	138.031573	206.26207	84	238
573	-30.22088	138.032071	208.106247	70	248
574	-30.220459	138.034572	218.40451	70	250
576	-30.220378	138.0351	220.685623	72	240
579	-30.24223	138.038185	237.836304	50	342
580	-30.243468	138.038412	224.108673	53	320
586	-30.244605	138.039264	226.956406	44	330
587	-30.247797	138.039747	241.042404	44	335
588	-30.247986	138.039765	241.788269	50	328
590	-30.248554	138.041669	253.249023	40	334
591	-30.249125	138.043255	268.421906	48	342
592	-30.24961	138.043629	275.603546	48	354
593	-30.25191	138.046245	347.260559	46	353
594	-30.253961	138.049727	432.917847	58	358
595	-30.252521	138.053381	410.916626	54	342
596	-30.250612	138.055145	303.661438	40	294
597	-30.250139	138.054748	288.510071	15	248
598	-30.248286	138.05259	269.286133	37	308
599	-30.246522	138.051275	258.963867	51	272
600	-30.245156	138.049405	263.463623	45	302
601	-30.245106	138.049542	278.06897	68	257
602	-30.244092	138.047269	238.289047	48	330
607	-30.221048	138.01883	205.723526	70	262
609	-30.237286	138.025317	201.972382	40	355
610	-30.236947	138.024839	198.949265	32	348
611	-30.23301	138.0227	202.566223	46	328
612	-30.232207	138.021365	201.516479	32	300
614	-30.214908	138.01792	168.561447	68	234
618	-30.212573	138.024707	197.679794	80	244
619	-30.212529	138.024919	200.202011	62	230
620	-30.212491	138.025808	204.807373	72	244
621	-30.212253	138.026276	202.047791	70	242
623	-30.214194	138.031458	219.568863	76	238
624	-30.214194	138.032278	226.062698	72	236
625	-30.213965	138.033021	227.152863	74	242
629	-30.274966	138.071337	160.802658	50	300

630	-30.269169	138.06984	165.604889		
631	-30.269077	138.069745	166.328339	60	270
632	-30.268659	138.069453	171.376236	72	78
633	-30.266995	138.068605	179.357834	84	64
634	-30.266268	138.068396	177.247498	80	78
635	-30.263159	138.068737	177.276764	74	72
636	-30.260751	138.068866	189.50441	44	236
637	-30.25897	138.067522	201.212006	44	256
638	-30.258906	138.066749	199.401001	76	238
639	-30.257847	138.064552	216.754028	62	248
640	-30.256663	138.063354	256.754242	30	330
641	-30.255849	138.064375	219.479187	82	250
642	-30.255582	138.06448	220.486084	52	282
643	-30.25482	138.065522	209.221664	84	77
644	-30.25227	138.064903	225.897263	20	252
645	-30.2516	138.065307	225.458328	42	220
646	-30.249445	138.063505	231.193115	42	282
647	-30.248795	138.0631	220.243866	60	268
648	-30.247844	138.062077	227.938477	60	255
649	-30.24409	138.060572	241.868042	72	266
650	-30.264335	138.071003	171.647644	40	260
651	-30.273823	138.067982	216.944122	42	62
653	-30.272968	138.067521	196.802185	52	70
654	-30.272501	138.067174	219.580185	40	16
655	-30.271373	138.067502	237.603058	78	56
656	-30.27109	138.067115	241.55545	56	45
657	-30.270514	138.066174	243.080307	56	20
658	-30.270114	138.065505	242.000488	64	6
659	-30.270157	138.064747	256.470123	62	350
660	-30.270016	138.064046	259.992065	65	20
661	-30.269762	138.063484	259.061035	53	12
662	-30.26993	138.062116	282.217163	48	15
663	-30.269852	138.061251	301.564087	40	16
664	-30.26879	138.057653	227.718491	54	336
665	-30.26839	138.057978	211.00145	48	350
666	-30.268017	138.058186	223.517014	34	334
667	-30.267612	138.05753	226.684128	42	324
668	-30.266939	138.056872	236.704834	48	353
669	-30.267012	138.054804	274.695099	61	52
670	-30.266612	138.053897	278.847198	62	52
671	-30.266337	138.053344	276.846313	72	2
672	-30.266183	138.051785	252.489716	58	20
673	-30.266539	138.051074	254.765472	32	2
674	-30.26669	138.050246	237.717148	52	304

675	-30.26678	138.04908	242.097626	54	320
676	-30.266505	138.048708	251.996445	50	30
677	-30.266235	138.048246	268.971924	42	344
678	-30.267217	138.047859	246.128632	63	267
679	-30.267923	138.047702	250.918243	72	276
680	-30.268355	138.047614	257.889832	58	228
681	-30.268944	138.047237	247.44104	53	296
682	-30.269744	138.047089	234.88269	86	264
683	-30.270929	138.04714	230.940857	80	272
684	-30.27146	138.047204	228.775192	66	243
686	-30.269859	138.053253	274.736847	40	40
687	-30.269931	138.053894	274.002625	40	15
688	-30.270212	138.054788	262.174805	54	32
689	-30.270531	138.055219	254.502945	60	44
690	-30.271832	138.057719	197.736511	58	36
691	-30.27207	138.058203	187.462646	74	38
693	-30.272637	138.059063	220.023605	66	13
694	-30.273074	138.060365	240.529922	79	8
695	-30.273184	138.060726	244.461609	40	12
696	-30.273657	138.061799	244.198883	58	23
697	-30.273799	138.062258	238.626862	38	17
698	-30.27394	138.063142	231.602585	50	20
699	-30.274438	138.06402	229.960022	52	25
700	-30.276673	138.056339	189.321152	70	40
701	-30.276257	138.05569	191.636093	76	220
702	-30.275128	138.054154	177.330002	80	236
703	-30.274568	138.053411	171.432022	66	214
704	-30.27406	138.052626	169.861282	76	236
705	-30.274872	138.052454	169.165237	80	43
706	-30.27517	138.052916	178.861008	68	30
707	-30.275924	138.053754	188.784241	80	43
708	-30.276754	138.055148	191.0569	70	46
709	-30.240936	138.038322	221.027695	64	322
711	-30.244624	138.045241	251.615997	64	276
712	-30.244984	138.045412	255.102814	58	272
713	-30.245511	138.049815	262.42337	26	287
714	-30.245222	138.050558	281.976044	50	267
715	-30.245336	138.051139	297.428528	62	260
716	-30.245481	138.051919	321.842041	64	256
717	-30.245598	138.052646	337.770172	54	262
718	-30.247311	138.052766	273.996857	52	255
719	-30.247621	138.052274	272.148254	65	278
720	-30.247731	138.052078	271.005615	40	300
721	-30.248126	138.050974	267.581299	52	340

722	-30.24804	138.050399	282.678284	42	346
724	-30.247581	138.049793	268.480194	30	330
725	-30.247363	138.049672	266.934204	42	6
726	-30.246881	138.049577	258.734436	46	346
727	-30.246186	138.049168	259.13623	42	340
728	-30.244722	138.046038	255.942032	54	350
729	-30.243766	138.044272	251.009949	52	286
730	-30.243453	138.043665	266.111084	70	300
731	-30.243308	138.04335	264.584442	68	284
733	-30.242833	138.041997	239.195572	36	270
734	-30.242269	138.041101	271.050903	58	298
735	-30.241156	138.039855	242.55896	58	290
736	-30.261901	138.0447	238.769836	64	302
739	-30.261728	138.046193	233.962601	40	326
740	-30.261798	138.046678	234.388245	40	332
741	-30.263393	138.048939	205.112	64	358
742	-30.262828	138.05013	219.620483	30	16
743	-30.263397	138.051554	218.821091	58	23
744	-30.262559	138.053388	223.893082	52	50
745	-30.263995	138.055506	223.962173	44	10
746	-30.264784	138.055982	223.172592	46	340
747	-30.264751	138.057298	231.033508	40	332
748	-30.264802	138.058923	255.494843	42	3
749	-30.264116	138.059183	256.391022	56	357
751	-30.263035	138.05869	256.135468	44	346
752	-30.262516	138.058561	279.496582	42	340
753	-30.261295	138.058945	325.75354	54	334
754	-30.261083	138.058532	321.205627	38	332
761	-30.260704	138.057849	332.99472	40	348
762	-30.259771	138.054926	262.102417	32	10
763	-30.259685	138.054249	273.505127	38	9
764	-30.259874	138.053586	297.832489	48	0
765	-30.259802	138.052887	309.714264	48	18
766	-30.259337	138.051945	296.342499	48	18
767	-30.258757	138.049603	273.958893	48	8
768	-30.258813	138.048784	306.21582	52	22
769	-30.257827	138.046381	304.904724	44	354
770	-30.257921	138.04489	312.12326	42	300
771	-30.251369	138.033262	199.588821	48	315
772	-30.24937	138.031402	222.289337	46	320
773	-30.248436	138.031963	229.068024	42	308
774	-30.021251	138.043188	168.493317	40	302

Table 8: Linciation readings

id#	Latitude	longitude	altitude	dip	dip direction
96	-30.2428	138.0412	286.6973	54	331
579	-30.2422	138.0382	237.8363	28	253
596	-30.2506	138.0551	303.6614	40	294

Table 9: Slicken line readings

id#	latitude	Longitude	altitude	dip	dip direction
630	-30.269169	138.06984	165.604889	60	130
685	-30.269839	138.050496	206.591263	36	256
701	-30.276257	138.05569	191.636093	30	192
600	-30.245156	138.049405	263.463623	18	20

Subarea data: subarea data is a series of subset groups of structural bedding readings from the field area and are grouped based on spatial difference. Grouped structural data is then plotted on Stereonet 9, based on algorithms described by (Cardozo & Allmendinger, 2013).

Table 10: Subarea 1 readings

subarea 1	
dip	strike
48	270
40	260
56	250
38	252
70	242
60	240
58	236
70	240
62	240
76	236
80	240
84	238
70	248
70	250

72	240
50	342
40	355
32	348
46	328
32	300
68	234
80	244
62	230
72	244
70	242
76	238
72	236
74	242

Table 11: Subarea 2 readings

subarea 2	
dip	strike
80	60
60	234
74	64
60	240
68	290
59	292
66	296
88	302
58	304
48	320
58	316
60	318
64	326
62	320
58	310
62	324
64	314
68	312
62	340
62	318
64	330
68	330
70	330
75	294
64	334
82	338

62	243
58	300
68	240
70	240
58	237
82	254
60	242
30	244
78	58
62	72
58	242
70	252
68	241
60	258
80	256
80	256
78	240
62	250
80	254
70	250
68	254
76	266
82	252
86	244
62	234
76	250
66	186
76	248
70	252
62	242
84	240
68	248
68	246
78	244
68	246
80	240
72	240
60	330
50	330
42	334
66	320
40	334
58	320
50	274

58	296
42	340
62	272
62	284
56	356
54	5
57	1
56	332
58	332
52	336
54	342
50	322
76	325
47	320
61	326
54	302
72	302
62	306
54	298
53	302
66	302
62	326
52	324
54	323
50	335
50	357
48	22
50	316
50	332
42	348
40	302
38	322
40	305
48	272
50	280
66	312
56	316
56	320
60	306
60	326
42	304
50	310
40	318
50	358

40	330
58	330
40	328
50	330
52	330
54	340
60	346
40	334
40	270
48	270
40	260
56	250
38	252
70	242
60	240
58	236
70	240
62	240
76	236
80	240
84	238
70	248
70	250
72	240
50	342
53	320
44	330
44	335
50	328
40	334
48	342
48	354
46	353
58	358
54	342
40	294
37	308
51	272
45	302
68	257
48	330
70	262
40	355
32	348

46	328
32	300
68	234
80	244
62	230
72	244
70	242
76	238
72	236
74	242
50	300
52	255
54	350
52	286
36	270
58	298
58	290
64	302

Table 12: Subarea 3 readings

subarea 3	
dip	strike
72	78
84	64
80	78
74	72
44	236
44	256
76	238
62	248
30	330
82	250
52	282
84	77
20	252
42	220
42	282
60	268
60	255
72	266
40	260

Table 13: Subarea 4 readings

subarea 4	
dip	strike
80	350
80	350
42	62
52	70
40	16
78	56
56	45
56	20
64	6
62	350
65	20
53	12
48	15
40	16
54	336
48	350
34	334
42	324
48	353
61	52
62	52
72	2
58	20
32	2
52	304
54	320
50	30
42	344
63	267
72	276
58	228
53	296
86	264
80	272
66	243
40	40
40	15
54	32
60	44
58	36

74	38
66	13
79	8
40	12
58	23
38	17
50	20
52	25
70	40
76	220
80	236
66	214
76	236
80	43
68	30
80	43
70	46

9.2 APPENDIX B: GEOCHRONOLOGY:

All U-Pb age data derived from iolite for each sample (W16-06, W16-07, W16-08, W16-09, W16-10), (Hellstrom et al., 2008).

Table 14: U-Pb data sample W16-06

Sample W16-06							
Analysis	Concordance %	Pb206/U238 (Ma)	Internal 2σ (Ma)	Propagated 2σ (Ma)	Pb ²⁰⁷ /Pb ²⁰⁶ (Ma)	Internal 2σ (Ma)	Propagated 2σ (Ma)
SS06-01.D	96.58966	1756	28	65	1818	52	72
SS06-02.D	81.58784	1449	29	57	1776	49	72
SS06-03.D	73.49138	1705	51	75	2320	110	120
SS06-04.D	93.09745	1605	30	61	1724	59	81
SS06-05.D	44.95798	1177	30	50	2618	41	65
SS06-06.D	104.7559	1674	26	60	1598	43	71
SS06-07.D	41.23711	720	16	29	1746	59	80
SS06-08.D	89.74082	1662	43	68	1852	82	99
SS06-09.D	99.12718	1590	20	57	1604	35	67
SS06-10.D	93.1677	1650	41	69	1771	75	94
SS06-11A.D	100.304	1650	42	69	1645	92	110
SS06-11B.D	89.29852	1744	42	72	1953	72	89
SS06-12.D	93.83736	1477	32	60	1574	72	91
SS06-13A.D	97.27346	1213	25	50	1247	68	87
SS06-13B.D	87.88796	1161	25	49	1321	79	99
SS06-14.D	78.58108	1163	50	64	1480	180	190
SS06-15.D	88.02608	1485	24	57	1687	33	62
SS06-16.D	92.10084	1096	18	43	1190	53	81
SS06-17.D	37.01578	774	23	36	2091	40	67
SS06-18.D	65.5102	1284	25	53	1960	50	71
SS06-19A.D	95.29101	1801	50	82	1890	110	120

SS06-19B.D	96.6532	1675	33	68	1733	76	93
SS06-20A.D	84.38662	1589	29	64	1883	53	76
SS06-20B.D	93.50877	1599	27	63	1710	57	79
SS06-21.D	84.36595	1457	25	58	1727	47	71
SS06-22.D	92.44521	1603	27	62	1734	51	75
SS06-23.D	97.59508	1745	28	66	1788	38	67
SS06-24.D	85.8871	1491	25	57	1736	53	76
SS06-25.D	94.84419	1674	31	65	1765	43	68
SS06-26.D	92.04301	1712	34	66	1860	54	75
SS06-27.D	86.91932	1422	22	53	1636	44	71
SS06-28.D	98.29868	1560	25	59	1587	39	67
SS06-29.D	89.88854	1129	20	43	1256	58	83
SS06-30.D	95.86957	1764	34	68	1840	62	82
SS06-31.D	91.89591	1236	20	47	1345	53	77
SS06-32.D	102.2606	1719	29	63	1681	42	70
SS06-33.D	89.42705	1514	31	59	1693	63	81
SS06-34.D	91.63253	1566	30	59	1709	58	79
SS06-35.D	88.58009	1753	38	69	1979	60	79
SS06-36.D	77.41652	881	15	34	1138	49	76
SS06-41.D	104.0127	1970	39	77	1894	56	78
SS06-42.D	79.31232	1384	42	65	1745	49	72
SS06-43.D	92.8737	1603	37	66	1726	67	85
SS06-44.D	97.05128	1514	30	60	1560	66	86
SS06-45.D	65.25709	1358	27	55	2081	56	77
SS06-46.D	94.12903	1459	35	60	1550	100	120
SS06-47.D	185.6061	9.80E+03	1.40E+03	1.40E+03	5280	480	500
SS06-48.D	65.0236	1240	36	54	1907	38	67
SS06-49.D	87.1583	1371	23	52	1573	62	81
SS06-50.D	94.26457	1019	18	39	1081	65	89

SS06-51A.D	80.06617	968	18	37	1209	65	86
SS06-51B.D	95.81422	1671	36	63	1744	43	69
SS06-52.D	99.58775	1691	34	64	1698	60	81
SS06-53.D	96.39588	1685	26	60	1748	45	69
SS06-54.D	82.49048	1517	25	55	1839	51	74
SS06-55.D	96.7128	1677	24	57	1734	45	70
SS06-56A.D	100.4142	1697	26	59	1690	53	74
SS06-56B.D	92.24664	1511	21	52	1638	33	64
SS06-57.D	101.833	1500	28	54	1473	49	75
SS06-58.D	89.97333	1687	31	60	1875	44	69
SS06-59.D	86.29808	1436	23	51	1664	35	65
SS06-60.D	93.38843	1017	22	39	1089	85	100
SS06-61.D	100.5115	1965	25	67	1955	26	57
SS06-62.D	100.3264	1537	29	57	1532	52	76
SS06-63.D	110.0204	1614	31	350	1467	63	86
SS06-64.D	92.65634	1615	40	2.10E+03	1743	98	110
SS06-65.D	104.6171	1858	32	-5.80E+04	1776	57	77
SS06-66.D	92.51899	1583	25	5.90E+03	1711	44	69
SS06-67A.D	100.4159	1690	37	1.60E+03	1683	79	95
SS06-67B.D	99.68454	1580	34	1.20E+03	1585	89	100
SS06-68.D	86.97454	1469	36	1.10E+03	1689	89	100
SS06-69.D	90.40853	1527	31	1.60E+03	1689	63	81
SS06-70A.D	91.29338	1447	27	3.30E+03	1585	65	84
SS06-70B.D	98.7797	1538	28	-2.90E+04	1557	65	82
SS06-71.D	99.61411	1807	32		1814	45	71
SS06-72.D	82.08868	1407	25	2.00E+03	1714	49	73
SS06-73.D	93.06393	1543	28	200	1658	41	64
SS06-74.D	93.43373	1551	36	150	1660	65	85
SS06-75.D	45.39978	829	28	83	1826	52	73

SS06-76.D	86.69456	1036	25	72	1195	87	110
SS06-77.D	95.92089	1552	29	87	1618	44	70
SS06-78.D	89.61456	1674	34	82	1868	57	77
SS06-79.D	97.90301	1494	28	69	1526	59	81
SS06-80.D	99.26862	1493	35	68	1504	85	99
SS06-81.D	96.15854	1577	37	69	1640	70	86
SS06-82	104.1466	1733	32	62	1664	43	120
SS06-83	75.5648	1271	26	48	1682	46	120
SS06-84	91.27124	1558	31	56	1707	61	130
SS06-85	76.28778	1792	37	66	2349	34	110
SS06-86	76.83673	1506	23	52	1960	26	110
SS06-87	67.4175	1287	39	55	1909	38	110
SS06-88	92.80042	1753	41	67	1889	72	130
SS06-89	98.50467	1581	29	56	1605	54	130
SS06-90	77.43902	1397	33	51	1804	58	110
SS06-91	96.1752	1559	24	54	1621	45	120
SS06-92	103.8163	1605	30	57	1546	52	130
SS06-93	78.04616	1454	25	51	1863	28	110
SS06-94	90.85873	1312	27	48	1444	67	140
SS06-95	98.98089	1554	35	58	1570	62	130
SS06-96A	101.1333	1874	31	65	1853	46	120
SS06-96B	84.97677	1646	33	60	1937	40	120
SS06-97	96.84075	1502	30	53	1551	69	140
SS06-98	89.65937	1474	29	54	1644	60	130
SS06-99	72.53086	1175	43	56	1620	140	180
SS06-100	83.77254	1812	42	68	2163	83	130
SS06-101	97.38611	1304	26	51	1339	80	150
SS06-102	86.25641	1682	66	90	1950	140	190
SS06-103	102.8518	1659	29	62	1613	45	130

SS06-104	98.75699	1589	40	67	1609	95	150
SS06-105	101.8129	1404	28	55	1379	60	130
SS06-106	89.05028	1594	45	71	1790	120	170
SS06-107	86.43976	1600	22	58	1851	31	110
SS06-108	85.75	1372	33	56	1600	82	140
SS06-109	91.5592	1562	33	62	1706	70	130
SS06-110	89.20692	1496	20	53	1677	37	120
SS06-111	88.28932	1538	34	61	1742	66	130
SS06-112	88.07786	1448	24	53	1644	51	130
SS06-113	95.9607	1758	27	62	1832	44	120
SS06-114	100.1125	1779	48	75	1777	88	140
SS06-115	79.52966	1488	29	55	1871	39	120
SS06-116	6.640731	196.3	9.1	11	2956	52	110
SS06-117	88.96383	1451	30	54	1631	42	120
SS06-118	95.07711	1603	33	60	1686	49	120

Table 15: U-Pb data sample W16-07

Sample W16-07							
Analysis	Concordance %	Pb206/U238 (Ma)	Internal 2σ (Ma)	Propagated 2σ (Ma)	Pb ²⁰⁷ /Pb ²⁰⁶ (Ma)	Internal 2σ (Ma)	Propagated 2σ (Ma)
SS07-1	94.60138	1507	26	54	1593	63	130
SS07-2A	99.21001	1507	33	58	1519	85	150
SS07-2B	88.69013	1537	29	56	1733	72	130
SS07-3	67.70538	2390	140	160	3530	180	210
SS07-4A	115.2995	1771	27	63	1536	49	130
SS07-4B	110.2696	1718	27	61	1558	45	120
SS07-4C	106.5272	1681	32	63	1578	50	120
SS07-5	102.0233	1664	27	61	1631	40	120
SS07-6A	101.7544	1566	37	64	1539	92	150

SS07-6B	92.98893	1512	25	55	1626	56	120
SS07-7	92.32456	2105	60	90	2280	98	140
SS07-8	100.618	1628	29	60	1618	59	130
SS07-9A	89.23952	1725	49	75	1933	93	140
SS07-9B	89.50586	1757	43	70	1963	84	140
SS07-10	63.26154	1028	21	40	1625	34	120
SS07-11	70.90113	1133	27	47	1598	57	120
SS07-12	60.39783	1002	19	38	1659	40	120
SS07-13A	108.48	271.2	6.8	11	250	100	160
SS07-13B	129.5238	272	13	16	210	180	210
SS07-14	92.28275	1423	27	52	1542	47	130
SS07-15	62.61378	963	25	39	1538	35	120
SS07-16A	94.21182	1530	31	56	1624	53	130
SS07-16B	94.906	1565	29	57	1649	52	130
SS07-17	66.19846	1461	39	60	2207	41	110
SS07-18A	104.1612	1577	35	61	1514	72	130
SS07-18B	91.92708	1412	26	52	1536	47	130
SS07-19	48.56335	1031	16	38	2123	31	110
SS07-20	99.12827	1592	29	58	1606	53	130
SS07-21	94.52991	1659	34	61	1755	61	130
SS07-22	98.58468	2020	31	67	2049	36	110
SS07-23	48.99536	951	27	40	1941	50	120

Table 16: U-Pb data sample W16-08

Sample W16-08							
Analysis	Concordance %	Pb206/U238 (Ma)	Internal 2σ (Ma)	Propagated 2σ (Ma)	Pb ²⁰⁷ /Pb ²⁰⁶ (Ma)	Internal 2σ (Ma)	Propagated 2σ (Ma)
SS08-1	79.61992	1215	22	76	1526	62	76
SS08-2	104.7619	1474	29	90	1407	74	86

SS08-3	103	1957	36	120	1900	43	59
SS08-4	107.9791	1651	29	100	1529	40	58
SS08-5	55.56685	1093	27	74	1967	48	63
SS08-6	98.89535	1701	61	120	1720	130	140
SS08-7	100	1678	29	100	1678	43	60
SS08-8	98.65196	1610	35	100	1632	79	91
SS08-9A	97.89006	1763	37	110	1801	58	72
SS08-9B	93.75679	1727	35	110	1842	59	71
SS08-10	96.59919	1193	27	80	1235	85	96
SS08-11	97.86566	1559	23	97	1593	34	54
SS08-12	-2.19	2190	210	250	-1.00E+05	2.40E+04	2.40E+04
SS08-13A	100.9988	1618	30	100	1602	70	83
SS08-13B	100.3785	1591	35	100	1585	69	82
SS08-14	100.6002	1676	35	110	1666	52	67
SS08-15	99.42434	2418	36	140	2432	26	48
SS08-16	55.47119	1242	25	81	2239	32	51
SS08-17	97.13805	1731	32	110	1782	41	58
SS08-18	59.80198	1812	40	110	3030	27	46
SS08-19	98.1775	2478	46	150	2524	39	53
SS08-20	92.7439	1521	50	100	1640	140	150
SS08-21	97.80362	1514	34	97	1548	68	81
SS08-22A	95.81431	1259	19	78	1314	39	59
SS08-22B	92.8047	1264	20	80	1362	51	68
SS08-23	84.58943	1504	27	94	1778	49	65
SS08-24A	72.06284	1055	24	70	1464	68	82
SS08-24B	84.10646	1106	31	76	1315	87	97
SS08-25A	76.76617	1543	49	100	2010	110	120
SS08-25B	92.56527	1631	42	100	1762	92	100
SS08-26	95.96879	1476	34	94	1538	84	94

SS08-27	79.65629	1715	35	110	2153	95	100
SS08-28	97.38255	1451	55	100	1490	160	170
SS08-29	94.21026	1855	29	110	1969	42	60
SS08-30	81.71123	1528	55	110	1870	120	120
SS08-31	94.91379	1101	29	74	1160	120	130
SS08-32	92.42726	2319	43	130	2509	39	54
SS08-33	58.94231	613	26	47	1040	190	190
SS08-34	29.30334	938	16	60	3201	33	49
SS08-35	33.44171	720	23	51	2153	68	78
SS08-36	97.49002	1709	30	100	1753	53	68
SS08-37	73.33333	1870	53	120	2550	110	110
SS08-38	95.90611	1757	35	110	1832	55	69
SS08-39	97.32591	1747	29	100	1795	45	61
SS08-40	104.0445	1029	18	65	989	57	74
SS08-41	96.74699	1606	28	97	1660	47	64
SS08-42	84.35518	1197	31	77	1419	86	96
SS08-43	83.12259	1512	43	98	1819	94	100
SS08-44	65.08772	1484	25	90	2280	55	68
SS08-45	43.5119	731	35	57	1680	210	210
SS08-46	28.05556	808	36	60	2880	120	130
SS08-47	86.62357	1742	46	110	2011	83	94
SS08-48	11.64166	256	21	24	2199	92	100
SS08-49	93.73892	1587	31	95	1693	59	72
SS08-50A	90.17186	1679	29	98	1862	59	72
SS08-50B	91.41469	1693	37	100	1852	71	82
SS08-51	91.93002	1629	33	98	1772	54	69
SS08-52A	98.25016	1516	32	92	1543	80	91
SS08-52B	103.0263	1566	40	97	1520	100	110
SS08-53A	91.31175	1608	28	95	1761	61	74

SS08-53B	95.52333	1515	31	91	1586	66	79
SS08-54	90.34722	1301	32	84	1440	120	130
SS08-55	106.5167	1847	30	110	1734	45	61
SS08-56	101.2926	1724	41	110	1702	71	83
SS08-57	99.42197	1548	37	97	1557	67	80
SS08-58	84.71517	1502	28	92	1773	53	68
SS08-59	101.3601	1714	37	110	1691	69	82
SS08-60	89.96599	1058	16	65	1176	43	63
SS08-61	60.74257	1227	21	75	2020	32	51
SS08-62	93.40426	1756	27	100	1880	42	58
SS08-63	88.27508	1566	37	97	1774	98	110
SS08-64A	82.03187	2059	36	120	2510	31	49
SS08-64B	96.87375	2417	35	130	2495	29	47
SS08-65	54.59459	1212	21	74	2220	49	60
SS08-66	93.82644	1611	32	97	1717	50	66
SS08-67A	62.16802	1147	29	75	1845	52	65
SS08-67B	54.88181	1068	22	67	1946	50	64
SS08-68	97.22402	1506	44	97	1549	92	100
SS08-69	96.85466	1786	33	100	1844	46	62
SS08-70	95.08111	1817	30	100	1911	47	62
SS08-71	93.27522	1498	33	92	1606	67	79
SS08-72	64.92199	1290	33	82	1987	83	93
SS08-73	98.21429	1760	35	100	1792	59	72
SS08-74	63.78698	1078	56	82	1690	210	210
SS08-75	99.22711	1669	30	97	1682	44	60
SS08-76	100.178	1688	30	99	1685	47	63
SS08-77	93.68296	1572	33	94	1678	80	88
SS08-78A	36.48586	787	25	53	2157	67	78
SS08-78B	95.03464	1646	37	98	1732	64	76

SS08-79A	93.97015	1574	30	92	1675	48	64
SS08-79B	98.00125	1569	39	97	1601	84	94
SS08-80	90.50461	1668	28	95	1843	35	55
SS08-81	95.81818	1581	45	95	1650	100	110
SS08-82	88.95487	1498	33	88	1684	52	67
SS08-83	97.11172	1782	35	100	1835	45	61

Table 17: U-Pb data sample W16-09

Sample W16-09							
Analysis	Concordance %	Pb206/U238 (Ma)	Internal 2σ (Ma)	Propagated 2σ (Ma)	Pb ²⁰⁷ /Pb ²⁰⁶ (Ma)	Internal 2σ (Ma)	Propagated 2σ (Ma)
SS09-1.D	105.2481	1103	22	28	1048	60	140
SS09-2.D	101.1681	1559	36	43	1541	75	140
SS09-3.D	86.76976	1515	24	34	1746	34	120
SS09-4A.D	100.6838	1767	27	40	1755	37	120
SS09-4B.D	99.48689	1745	32	44	1754	56	130
SS09-5A.D	97.19811	2463	44	58	2534	46	110
SS09-5B.D	74.10678	1846	40	49	2491	47	110
SS09-6.D	99.35065	1683	30	40	1694	50	130
SS09-7.D	88.68753	1615	42	49	1821	50	120
SS09-8.D	100.5744	1751	31	42	1741	47	130
SS09-9.D	95.43773	1548	35	43	1622	73	140
SS09-10A.D	90.06041	1640	32	42	1821	67	140
SS09-10B.D	95.20468	1628	24	35	1710	35	120
SS09-11.D	88.97119	1081	27	32	1215	84	150
SS09-12.D	96.70588	1644	37	45	1700	81	140
SS09-13.D	88.82387	1518	29	39	1709	45	130
SS09-14.D	58.29089	1030	19	25	1767	34	120
SS09-15.D	94.89583	911	16	22	960	55	130

SS09-16.D	94.48385	2398	36	52	2538	33	110
SS09-17A.D	93.63208	1985	31	45	2120	38	120
SS09-17B.D	89.78723	1899	36	48	2115	38	120
SS09-18.D	99.7669	1284	23	31	1287	47	130
SS09-19.D	97.7425	2771	48	63	2835	32	110
SS09-20.D	91.44089	1485	39	46	1624	87	150
SS09-21.D	95.96727	1642	32	42	1711	55	130
SS09-22.D	92.72951	1505	35	42	1623	61	130
SS09-23.D	96.4881	1621	38	46	1680	83	140
SS09-24A.D	92.94574	1199	33	38	1290	110	170
SS09-24B.D	103.8211	1277	33	39	1230	110	170
SS09-25.D	83.64929	1059	22	28	1266	53	130
SS09-26.D	89.91453	1052	35	41	1170	140	190
SS09-27A.D	95.52752	1666	36	45	1744	67	140
SS09-27B.D	96.51163	1660	36	45	1720	69	140
SS09-28.D	96.16667	1154	36	42	1200	120	180
SS09-29.D	73.65743	1303	27	37	1769	49	120
SS09-30.D	99.67554	1536	28	37	1541	52	130
SS09-31.D	96.54545	1593	30	40	1650	52	130
SS09-32.D	101.1992	1519	40	47	1501	86	150
SS09-33.D	95.89443	1635	36	44	1705	73	140
SS09-34.D	97.4307	1441	31	39	1479	73	140
SS09-35A.D	96.52695	1612	30	40	1670	40	120
SS09-35B.D	89.41245	1537	26	35	1719	37	120
SS09-36A.D	100.8996	673	14	19	667	94	160
SS09-36B.D	96.08392	687	17	21	715	90	160
SS09-37.D	94.59295	1557	31	39	1646	65	130
SS09-38.D	100.0633	1582	26	38	1581	48	130
SS09-39.D	98.07916	1685	30	42	1718	52	130

SS09-40.D	95.69892	1958	38	48	2046	51	120
SS09-41.D	90.26688	1150	18	26	1274	46	130
SS09-42A.D	96.04694	1555	32	41	1619	60	130
SS09-42B.D	97.1831	1518	30	38	1562	44	120
SS09-43.D	98.96492	1721	32	43	1739	54	130
SS09-44.D	90.40493	1027	17	24	1136	44	140
SS09-45.D	66.09393	1154	25	31	1746	40	120
SS09-46.D	67.01657	1213	44	49	1810	110	160
SS09-47.D	93.2008	2344	34	48	2515	34	110
SS09-48.D	47.76589	759	14	19	1589	35	120
SS09-49.D	68.0203	1206	21	30	1773	34	120
SS09-50.D	96.63659	1178	29	35	1219	76	140
SS09-51.D	100.0677	1478	26	36	1477	56	130
SS09-52.D	99.59112	1705	28	39	1712	46	130
SS09-53.D	85.15573	1285	27	34	1509	40	130
SS09-54.D	88.22184	1543	26	36	1749	34	120
SS09-55.D	96.15699	1176	24	31	1223	57	130
SS09-56A.D	84.54318	1351	34	40	1598	85	150
SS09-56B.D	98.79241	1718	40	49	1739	74	140
SS09-57.D	16.52363	265.7	7.6	9.4	1608	45	120
SS09-58.D	97.31844	1742	26	39	1790	39	120
SS09-59.D	93.7818	1659	36	44	1769	66	140
SS09-60.D	101.9988	1735	35	45	1701	69	140
SS09-61.D	88.23821	1778	40	49	2015	71	140
SS09-62A.D	97.01789	1464	24	34	1509	39	130
SS09-62B.D	92.48408	1452	27	36	1570	54	130
SS09-63.D	97.806	1694	29	39	1732	50	130
SS09-64.D	99.76676	1711	28	41	1715	45	120
SS09-65.D	101.8304	1057	20	26	1038	61	140

SS09-66.D	100.4548	1546	37	44	1539	73	140
SS09-67.D	96.75	1161	35	40	1200	120	170
SS09-68.D	101.0084	1202	22	31	1190	52	140
SS09-69.D	95.19704	1546	41	49	1624	91	150
SS09-70.D	89.68668	1374	31	40	1532	60	130
SS09-71.D	96.82741	1526	37	46	1576	84	140
SS09-72.D	96.68593	2509	50	67	2595	40	110
SS09-73.D	117.6289	1141	30	35	970	120	170

Table 18: U-Pb data sample W16-10

Sample W16-10							
Analysis	Concordance %	Pb206/U238 (Ma)	Internal 2σ (Ma)	Propagated 2σ (Ma)	Pb ²⁰⁷ /Pb ²⁰⁶ (Ma)	Internal 2σ (Ma)	Propagated 2σ (Ma)
SS10-1.D	108.3255	1158	28	29	1069	75	91
SS10-2.D	88.60688	1571	33	35	1773	73	86
SS10-3.D	98.98305	1168	31	32	1180	110	120
SS10-4A.D	100.5808	1039	26	28	1033	93	100
SS10-4B.D	94.4186	1015	29	30	1075	93	110
SS10-4C.D	95.00471	1008	26	27	1061	82	94
SS10-5.D	104.4237	1676	34	37	1605	56	72
SS10-6.D	90.34974	1395	26	29	1544	37	60
SS10-7.D	102.904	1630	35	38	1584	65	80
SS10-8.D	98.34559	1605	32	34	1632	55	73
SS10-9.D	90.46599	1689	44	46	1867	86	96
SS10-10.D	93.38118	1171	21	23	1254	51	70
SS10-11.D	85.1513	1210	26	28	1421	84	95
SS10-12.D	106.2668	1187	24	26	1117	70	86
SS10-13.D	107.5972	1218	26	28	1132	80	93

SS10-14.D	97.11599	1549	27	30	1595	45	65
SS10-15.D	88.20929	1197	29	31	1357	88	99
SS10-16.D	103.2358	1659	31	34	1607	45	65
SS10-17.D	96.76214	1554	30	33	1606	51	69
SS10-18.D	69.50473	1249	29	31	1797	82	93
SS10-19.D	102.3028	1777	30	34	1737	42	62
SS10-20.D	89.64346	1584	31	34	1767	51	70
SS10-21.D	34.46009	734	27	28	2130	130	140
SS10-22.D	62.62376	1265	42	43	2020	120	120
SS10-23.D	90	1017	26	28	1130	100	120
SS10-24.D	99.53569	1715	30	33	1723	45	65
SS10-25.D	86.51207	1828	36	39	2113	63	76
SS10-26.D	90.84112	972	26	28	1070	120	130
SS10-27.D	99.38272	1771	39	42	1782	63	78
SS10-28.D	102.9569	2507	38	43	2435	35	56
SS10-29.D	93.1746	1174	26	29	1260	77	91
SS10-30.D	102.5573	2687	45	50	2620	33	52
SS10-31A.D	104.2697	928	21	23	890	110	120
SS10-31B.D	68.90323	1068	38	39	1550	130	130
SS10-32A.D	97.61364	859	28	29	880	140	150
SS10-32B.D	87.95699	818	37	38	930	190	200
SS10-33.D	63.58253	859	14	16	1351	36	60
SS10-34A.D	105.6769	1694	42	45	1603	80	93
SS10-34B.D	94.35984	1673	35	38	1773	54	69
SS10-35A.D	103.1707	846	27	29	820	130	140
SS10-35B.D	104.9383	850	27	28	810	140	150
SS10-36.D	103.3947	1797	34	39	1738	45	65
SS10-37.D	98.03013	1692	32	35	1726	55	72
SS10-38.D	101.8556	2031	51	54	1994	80	88

SS10-39.D	102.2981	1558	36	39	1523	77	91
SS10-40.D	103.8559	1643	32	36	1582	49	69
SS10-41.D	89.55793	1175	23	25	1312	58	77
SS10-42.D	101.2048	840	26	27	830	120	130
SS10-43.D	102.3553	1521	32	35	1486	67	82
SS10-44.D	90.97801	1200	25	27	1319	62	78
SS10-45.D	99.40793	1679	27	31	1689	45	64
SS10-46A.D	100.7018	1148	35	37	1140	110	120
SS10-46B.D	109.3204	1126	38	39	1030	110	130
SS10-47.D	86.17284	698	40	41	810	280	280
SS10-48.D	61.73267	1247	22	25	2020	31	54
SS10-49.D	97.38448	1117	23	26	1147	71	86
SS10-50.D	99.52747	1685	27	31	1693	42	63
SS10-51.D	94.74758	1858	34	38	1961	44	62
SS10-52.D	102.6159	863	17	19	841	68	85
SS10-53.D	93.60873	1201	23	25	1283	61	79
SS10-54A.D	103.0164	1571	35	38	1525	68	83
SS10-54B.D	98.54522	1558	30	33	1581	53	70
SS10-55A.D	102.0175	1163	31	32	1140	110	120
SS10-55B.D	99.91297	1148	24	27	1149	86	100
SS10-56.D	100.1161	1724	35	38	1722	63	77
SS10-57A.D	81.42857	684	22	23	840	140	140
SS10-57B.D	90.78947	690	17	18	760	110	120
SS10-58.D	98.62328	1576	34	37	1598	66	81
SS10-59.D	95.47988	1542	33	36	1615	53	71
SS10-60.D	65.10721	1002	24	26	1539	69	84
SS10-62.D	80.07299	1097	35	36	1370	110	120
SS10-63.D	95.53806	1092	21	23	1143	65	82
SS10-64A.D	79.73856	1220	37	39	1530	130	140

SS10-64B.D	90.40785	1197	31	33	1324	79	91
SS10-65A.D	92.05882	1565	42	44	1700	83	94
SS10-65B.D	92.36408	1512	41	43	1637	98	110
SS10-66.D	101.7029	1732	25	30	1703	34	58
SS10-67.D	99.26963	1631	30	34	1643	57	73
SS10-68.D	91.10345	1321	33	35	1450	95	100
SS10-69.D	102.1875	654	11	13	640	68	87
SS10-70.D	96.42586	1268	25	27	1315	58	74
SS10-71.D	96.85039	1599	27	31	1651	37	60
SS10-72.D	100.3279	1224	41	42	1220	140	150
SS10-73.D	99.06701	1168	22	25	1179	66	82
SS10-74A.D	84.41843	1154	25	27	1367	68	82
SS10-74B.D	88.15277	1131	23	25	1283	59	77
SS10-75.D	88.58785	1079	19	21	1218	46	67
SS10-76A.D	92.18935	1558	57	59	1690	130	140
SS10-76B.D	90.73446	1606	53	55	1770	110	120
SS10-77.D	95.67504	1637	34	37	1711	52	67
SS10-78A.D	87.79221	676	17	19	770	100	110
SS10-78B.D	111.4286	702	21	22	630	130	140
SS10-79.D	80.74041	1832	52	54	2269	89	99
SS10-80.D	95.2919	1518	28	31	1593	39	61
SS10-81.D	86.73797	811	19	21	935	89	100
SS10-82A.D	87.33372	1510	31	34	1729	55	71
SS10-82B.D	94.85512	1604	34	37	1691	52	70
SS10-83A.D	85.76389	1482	33	35	1728	66	80
SS10-83B.D	98.41672	1554	27	31	1579	51	69
SS10-84.D	95.63523	1227	23	26	1283	54	72

Multi-Dimensional Scaling data: MDS data is in the form of Pb207/Pb206 or Pb206/U238 ages (Ma), with respective error for each analysed province region (Gawler Craton, Musgrave Block and Curnamona Craton). Gawler Craton data is taken from analysis by (Belousova et al., 2006; Fraser & Neumann, 2010; Howard, 2006), Musgrave data is taken from analysis by (Wade et al., 2008) and Curnamona Craton data is taken from analysis by (Fraser & Neumann, 2010).

MDS is done in the free program “R” with a specific provenance package. Details on modelling data are provided by (Vermeesch et al., 2016).

Table 19: Gawler Craton provenance data

Gawler Craton			
Pb207/Pb206	$\pm 1\sigma$	Pb206/U238	$\pm 1\sigma$
2077	18	1959	21
2051	18	1933	18
2078	18	1885	20
2517	17	2422	24
2002	18	1879	19
2025	18	1894	19
2463	17	2350	23
2069	18	1865	17
2013	18	1873	19
2017	18	1940	18
2182	18	2396	24
2459	17	2305	22
1935	19	1752	19
2175	18	2082	21
1898	19	1709	17
1881	18	1851	20
1983	18	1836	18
2506	17	2408	24
1992	18	1911	21
1898	18	1837	19
2022	18	1861	20
2050	19	1999	21
2033	19	1876	20
1968	18	1882	19
1906	20	1909	18
1993	20	1891	18
2009	19	1819	19
2124	21	1954	21
2047	19	1913	21
1971	18	1912	19
2453	18	2202	23

1882	20	1873	20
1988	19	1927	19
2022	19	1834	20
2444	17	2397	23
2428	17	2239	22
2170	18	1971	21
2020	18	1973	20
2051	18	1991	20
1999	19	1823	21
1927	18	1926	21
2483	17	2365	23
2012	21	1801	16
2440	17	2309	24
1995	18	1868	18
1987	18	1839	19
2486	18	2428	23
2018	18	1967	19
2070	20	1875	21
2769	16	2757	25
2016	18	1945	19
2021	18	1959	19
2413	17	2374	23
1990	18	1971	20
1978	18	2012	21
1951	18	1962	20
1946	18	1882	19
2511	17	2410	26
2533	18	2451	22
2403	17	2346	24
1980	18	1995	20
2425	18	2212	22
2121	18	1922	19
2201	19	2127	20
2503	17	2390	24
2508	17	2417	23
2506	18	2379	25
2663	20	2668	29
2066	18	1982	20
2091	19	1965	20
2556	17	2288	24
1998	18	1932	20

2050	18	1908	22
2442	19	2294	23
2596	19	2400	25
2356	19	2109	24
1985	20	1934	20
2505	17	2418	26
2319	18	2214	23
2626	17	2368	24
2656	17	2512	25
1887	20	1766	19
2499	17	2294	23
1852	18	1659	18
1877	18	1788	18
1997	18	1893	19
1984	20	1954	20
2469	18	2390	24
1899	20	1896	21
1992	18	1911	20
1870	19	1855	20
2172	18	2160	24
2435	17	2334	24
1987	18	1963	20
2349	19	2266	26
2057	21	1931	23
1967	18	1894	22
1978	20	2012	25
1997	19	1949	22
1990	20	1865	21
1990	19	1889	21
2000	19	1926	22
1886	18	1890	20
1952	19	1935	22
1976	18	1940	21
2068	19	1967	23
1903	18	1839	20
1925	18	2019	21
1942	19	1867	22
1915	20	1923	21
2447	17	2379	24
1979	18	1972	21
1893	18	1899	22

1908	19	1762	20
1903	18	1871	21
1965	18	1962	22
2603	17	2343	24
2533	17	2504	30
2533	17	2439	27
2521	17	2483	27
2532	17	2510	26
2665	17	2591	28
2523	18	2411	32
2702	17	2612	30
2518	17	2438	27
2552	17	2318	26
2523	17	2456	27
2519	17	2458	30
2519	17	2355	28
2004	18	2015	23
2034	21	1992	21
2016	18	2010	23
2004	18	2041	23
2026	18	2030	22
2005	20	2033	24
2019	19	1986	23
2068	18	1953	22
2020	23	2058	30
2090	22	1912	20
2030	19	1950	21
2037	20	1959	25
2010	20	2006	23
2019	18	2013	24
2023	19	2035	22
2004	18	1978	22
1055	21	1016	13
1183	33	1110	15
1983	20	1874	22
2006	19	1946	23
1174	25	1096	14
2009	21	1942	25
1176	23	1116	14
1202	23	1152	14
2028	18	2010	25

2000	19	1891	22
1997	21	1962	25
2024	19	1929	22
2015	19	1928	22
1068	29	974	12
1626	23	1557	19
1306	22	1270	16
1693	28	1551	22
2621	18	2568	30
1172	29	1079	14
1591	21	1569	16
1658	20	1536	15
1598	20	1547	15
1577	19	1558	15
1579	20	1577	16
1588	20	1543	16
1591	57	1585	19
1586	19	1596	16
1590	20	1544	16
1616	21	1549	17
1583	19	1577	16
1592	20	1579	16
1647	21	1587	17
1724	19	1709	18
1574	26	1577	18
1574	21	1595	17
1585	20	1571	16
2635	17	2638	25
1581	22	1595	17
1696	20	1543	16
1576	22	1578	17
1596	21	1567	16
1608	21	1561	16
1658	22	1531	16
1652	21	1484	15
1573	22	1604	16
1723	18	1654	17
1898	19	1740	17
1731	19	1715	17
1671	21	1668	17
1613	20	1609	17

1722	21	1708	18
1594	25	1600	18
2412	17	2346	23
1613	20	1494	15
1667	19	1526	15
1574	21	1574	16
1626	21	1586	16
1841	19	1803	15
1559	38	1600	14
1691	26	1705	15
2540	25	2553	24
1888	17	1916	15
1733	24	1632	14
2436	23	2347	18
2362	16	2286	16
1823	18	1798	17
2635	17	2604	24
1801	19	1778	19
2536	18	2364	23
2597	17	2394	24
1620	19	1580	16
2545	17	2319	21
1623	20	1534	15
1571	20	1517	16
1616	20	1529	16
1584	21	1524	16
1712	18	1694	17
1612	19	1577	16
1572	20	1523	16
1836	19	1751	18
2506	18	2443	26
2443	17	2384	23
1751	19	1630	17
2502	17	2432	24
1901	18	1858	19
2447	18	2337	22
1720	20	1681	17
2400	39	2353	25
2359	17	2315	23
2469	17	2450	23
1778	19	1813	19

2456	17	2431	25
2760	17	2521	24
2445	17	2377	23
1733	20	1674	18
1743	19	1700	17
1746	19	1714	18
1812	19	1758	18
1723	21	1696	18
2453	18	2458	25
1757	19	1739	18
1557	19	1516	16
1751	19	1723	18
3171	35	3047	33
1789	18	1754	18
2660	19	2614	29
1724	19	1701	18
2449	30	2370	24
1839	18	1904	22
2456	18	2461	28
2416	17	2404	25
1716	20	1658	18
2408	43	2382	27
1570	22	1535	17
2409	17	2318	26
1772	19	1757	19
1781	19	1763	19
1870	19	1869	21
1618	19	1651	18
1610	36	1460	16
1762	19	1761	19
1751	19	1767	19
1762	18	1791	19
1838	18	1864	20
1750	19	1727	19
2671	39	2476	29
1731	18	1713	18
1872	19	1866	20
1750	18	1753	19
1751	18	1748	18
1748	18	1733	18
1624	40	1523	17

1762	19	1754	19
1664	20	1632	18
1893	19	1869	20
1886	18	1898	20
1709	20	1681	20
1733	19	1708	19
1784	19	1777	19
1714	19	1689	19
1600	20	1586	18
1785	19	1762	20
1983	18	1992	21
1728	19	1747	20
2010	18	2021	22
1749	19	1752	19
1857	18	1898	21
1699	18	1702	19
1847	18	1810	20
2760	17	2557	27
1789	19	1766	19
1781	19	1772	19
1782	21	1721	20
2366	17	2358	25
1747	19	1578	19
1768	21	1777	20
1732	19	1697	18
1738	19	1755	19
1778	20	1749	19
2035	61	2046	27
1846	18	1849	20
1638	22	1647	18
2078	45	2048	24
2878	16	2770	28
1771	19	1772	20
1868	18	1867	20
2016	18	1948	21
1625	19	1610	17
1768	19	1746	19
2874	32	2631	28
1674	22	1581	18
2140	18	2100	23
1595	20	1589	18

3179	16	3051	31
3022	35	2772	33
1982	18	1904	21
1691	19	1700	19
1736	19	1769	21
2249	19	2246	25
2008	18	1969	22
1791	22	1673	20
1734	20	1717	18
2809	16	2742	26
2497	17	2242	21
2540	18	2500	26
2523	17	2515	24
2922	16	2948	27
2588	21	2387	27
2514	17	2317	24
2436	18	2426	26
2519	17	2490	24
2588	17	2552	25
2366	17	2255	22
2478	17	2311	23
2524	17	2338	23
2508	17	2349	23
1752	24	1662	18
2506	17	2411	23
2645	31	2567	25
1730	21	1699	17
2608	18	2541	25
2479	37	2400	25
2545	17	2457	24
2657	32	2472	25
2550	17	2508	24
2538	17	2469	24
2599	20	2522	26
2767	16	2616	25
2805	101	2583	47
2476	17	2413	23
3214	28	3032	29
1643	55	1667	19
3193	32	3058	31
2453	17	2259	22

2410	17	2407	25
1559	87	1596	21
2562	18	2458	24
2456	17	2401	23
2493	17	2430	24
2533	17	2277	22
1699	20	1650	17
2521	32	2346	24
2554	16	2333	22
2521	33	2437	25
3127	34	2945	32
3162	28	3001	29
2480	17	2337	23
2600	18	2446	25
2460	18	2440	25
2483	17	2442	24
1716	22	1699	17
2535	20	2494	27
2440	18	2426	23
1725	20	1755	17
1873	19	1882	18
1739	19	1751	18
2457	20	2409	23
2435	19	2429	23
1989	19	1939	19
1847	19	1877	19
1858	19	1855	19
1753	20	1746	17
2831	30	2611	26
1732	19	1772	18
2006	19	2010	22
1830	18	1830	20
1885	19	1860	20
1727	20	1772	19
1756	19	1792	18
1836	18	1853	19
3097	16	3027	28
1841	39	1803	19
1742	19	1705	19
2035	18	1956	20
1723	47	1721	19

1739	19	1738	17
1987	18	1977	20
1784	45	1805	20
2024	18	1955	19
1743	19	1737	19
2811	17	2762	28
1849	20	1878	21
2053	18	1968	21
1999	19	2065	23
2008	19	2001	21
1904	18	1894	20
2025	18	2046	21
3135	16	3067	30
1759	19	1707	18
1753	19	1764	19
3068	16	3022	29
2133	18	2079	23
2008	18	2030	21
1899	18	1818	19
3079	16	3015	30
1885	19	1877	20
1703	19	1718	18
1860	19	1861	20
2030	18	1955	19
2034	18	2011	19
2035	19	1990	19
2028	18	2009	19
2044	19	2006	19
2021	18	2022	20
2025	21	1904	21
1732	20	1776	18
2017	18	1999	19
2026	21	1882	18
2018	18	1985	19
1848	19	1844	18
2028	18	2030	19
2026	19	2012	19
2382	19	2153	23
2027	21	1951	18
1998	21	1996	21
2017	19	2023	19

1902	56	1930	22
2016	18	1975	20
2025	18	1935	19
2000	18	1917	20
2000	39	1938	20
2457	18	2348	23
1996	19	1935	19
1831	20	1728	20
2011	18	1955	19
2014	18	1935	20
2021	18	1989	20
2029	18	1986	21
2028	18	1988	20
2015	18	1988	20
2028	18	2000	21
2022	18	1928	21
2010	18	2020	21
1967	19	2111	21
2025	18	1957	20
2023	18	1833	19
2026	18	1980	21
2028	18	2028	21
1979	46	1962	23
1828	60	1777	22
1829	53	1747	21
2527	19	2528	28
1763	28	1748	23
2032	20	1935	23
2436	17	2444	27
1783	18	1750	20
2033	19	2036	23
1856	20	1859	22
1877	18	1807	21
2018	19	2007	23
1938	19	1917	22
2001	19	1954	20
2044	18	2000	20
2024	18	2000	20
2017	20	1937	21
2020	21	1991	22
1749	19	1703	19

2446	17	2424	24
1775	19	1776	19
2017	18	2016	21
1852	19	1737	20
2021	19	2034	21
2022	21	2045	22
1888	18	1841	19
2039	19	2049	22
2049	19	2035	22
2040	18	2042	21
2358	17	2309	24
2029	18	2006	22
2031	18	1973	21
2441	17	2397	24
2001	19	2041	22
2011	18	2052	22
2048	18	1985	20
2010	19	2030	21
1854	18	1872	20
2011	18	1930	20
2022	19	2030	22
2038	19	2050	23
2050	19	2041	21
2038	19	2040	22
2041	18	1964	21
2039	18	2078	22
2029	18	2034	21
2019	19	2057	22
1855	18	1858	21
2424	16.5	2303	22.5
2017	18	2010	21
1848	18	1777	19
2508	16	2503	24
1868	18	1859	19
2017	18	1999	20
2013	18	2011	20
2007	18	1994	20
2694	17	2671	21
1712	40	1624	15
1600	29	1606	15
3143	16	3147	23

1905	19	1848	15
3136	20	2850	28
2475	18	2481	22
2505	18	2536	18
2503	18	2406	17
3231	16	3043	22
2853	18	2801	19
3136	16	3142	22
1805	26	1713	14
1664	22	1638	13
2492	20	2477	19
2692	18	2631	23
2493	18	2443	22
2536	18	2573	20
3008	16	2963	20
1705	20	1706	14
3061	17	3002	21
1751	21	1758	13
1644	47	1541	14
1557	31	1590	16
3232	16	3231	23
3220	17	3218	22
1639	20	1621	13
3188	16	3167	22
2491	18	2476	19
2478	18	2439	18
1558	26	1560	13
2956	17	2946	21
1755	20	1627	13
1743	21	1763	14
1696	20	1676	13
1696	19	1690	13
1836	22	1791	14
1751	23	1679	14
1678	21	1582	14
2245	19	2218	17
1819	19	1750	16
1711	23	1560	13
1699	20	1714	14
1709	22	1628	13
1684	22	1674	13

1694	21	1571	13
1684	20	1542	13
1681	19	1634	13
1654	21	1610	13
1752	21	1713	14
1693	20	1717	14
1815	22	1689	13
1895	22	1808	16
1600	46	1615	18
1672	31	1636	15
3149	17	3131	23
1683	23	1581	14
1680	21	1649	15
1615	21	1585	16
2256	18	2247	18
1731	23	1723	15
1639	21	1633	14
1646	33	1639	18
1649	20	1590	14
1782	21	1796	15
1667	21	1570	14
1740	20	1727	14
1550	24	1513	13
1589	20	1593	15
1523	22	1528	13
1636	20	1524	13
2817	16	2779	22
2646	18	2649	25
1658	58	1640	17
1641	22	1628	16
1755	20	1801	16
1880	21	1895	16
1577	21	1552	15
2476	19	2508	21
2436	18	2451	21
1715	22	1695	16
2562	34	2485	25
1770	20	1753	16
1660	72	1636	19
2147	19	2143	17
1621	22	1629	16

2478	19	2468	24
1826	23	1806	15
1753	25	1748	16
2452	20	2468	20
2862	16	2988	24
1769	23	1742	19
2416	19	2444	20
2387	27	2337	21
2447	19	2500	25
2467	19	2447	19
1668	20	1767	16
2454	19	2448	20
2456	20	2418	20
2421	18	2438	19
2293	18	2148	16
2488	17	2228	16
2427	17	2361	17
2440	21	2362	23
2444	17	2447	21
2464	17	2378	18
2450	17	2481	20
2454	17	2464	18
2450	18	2462	24
2507	18	2500	20
2460	17	2420	19
1685	30	1686	16
2427	18	2327	20
2441	17	2451	21
1846	19	1868	15
2476	18	2435	20
2413	17	2396	20
2483	20	2442	21
2414	17	2399	18
2458	17	2434	19
1719	21	1686	14
2675	21	2665	25
1848	62	1687	19
1727	47	1709	22
2389	18	2334	18
1719	21	1584	14
2345	21	2271	16

2385	17	2171	17
1719	29	1687	15
1694	22	1653	14
2415	18	2386	18
1787	38	1703	20
2409	18	2377	19
2354	18	2202	17
1674	19	1676	13
2262	21	2209	19
1705	23	1702	16
1797	52	1720	25
1717	22	1710	16
1758	19	1749	14
2376	18	2302	18
2463	21	2409	21
1530	21	1512	14
2469	20	2471	21
1707	23	1704	14
1714	25	1718	15
2466	18	2433	19
2462	18	2389	19
2035	21	1909	15
1844	37	1744	17
2451	19	2468	20
2466	18	2453	20
1604	19	1581	13
2424	30	2358	21
2249	18	2090	16
2447	18	2426	18
2428	18	2465	19
2453	18	2426	18
2328	18	2317	19
2430	19	2438	20
1579	27	1563	14
2431	18	2388	18
2427	19	2472	20

Table 20: Musgrave Block provenance data

Musgrave Block			
Pb207/Pb206	$\pm 1 \sigma$	Pb206/U238	$\pm 1 \sigma$
1696	54	1702	26

1534	53	1361	29
1665	24	1578	31
1472	46	1450	43
1669	25	1646	26
1602	143	1059	17
1616	57	1502	35
1623	31	1447	20
1361	194	1544	39
1162	39	1147	27
1587	29	1539	19
1573	34	1568	24
1799	24	1696	20
1559	36	1648	34
1527	58	1585	42
1195	55	1108	31
1215	20	1149	15
1485	25	1363	21
1609	26	1640	28
1646	44	1572	32
1493	47	1400	33
1267	61	1247	43
1220	32	1122	29
1245	120	1166	32
1240	43	1177	22
1555	35	1536	17
1532	24	1569	21
1586	21	1427	19
1465	44	1345	19
1543	19	1440	39
1581	13	1516	35
1541	23	1542	30
1099	58	1133	21
1503	28	1332	23
1145	29	1097	27
1592	21	1481	38
1190	35	1134	23
1655	47	1533	26
1576	32	1450	14
1644	21	1602	30
1453	48	1253	29
1401	36	1403	30
1404	71	1305	18
1584	20	1536	14

1549	19	1438	21
1490	20	1359	14
1600	20	1436	25
1647	25	1298	25
1641	22	1576	24
1410	32	1232	50
1553	21	1426	32
1694	30	1662	14
1637	26	1534	17
1533	28	1361	20
1486	41	1374	27
1596	57	1588	49
1578	31	1606	39
1759	45	1751	24
1740	11	1707	13
1424	75	1289	17
1302	68	1226	13
1274	12	1214	10
1914	30	1761	19
1754	10	1686	13
1742	20	1600	15
1543	16	1473	17
1640	19	1600	16
1725	13	1628	13
1444	33	1287	16
1837	18	1797	19
1721	15	1652	16
1686	14	1549	16
1524	23	1477	13
1817	27	1785	16
1711	38	1724	19
1644	12	1566	13
1529	22	1476	13
1956	9	1937	16
1736	14	1865	17
2373	32	1964	20
1166	21	1150	12
1639	39	1578	20
1256	15	1214	10
1762	17	1749	19
1632	13	1541	13
1647	8	1541	11
1613	40	1580	19

1871	34	1944	15
1732	15	1769	14
1687	10	1783	30
1730	11	1740	12
1160	35	1199	12
1201	7	1207	9
1752	36	1898	19
2736	6	2935	23
1649	16	1564	14
1762	20	1721	14
1579	35	1375	14
1649	18	1481	11
1583	10	1490	11
1940	18	1848	16
1295	28	1472	11
1295	28	1263	11
1672	13	1630	15
1768	28	1826	13
1712	24	1833	16
1712	24	1645	14
1842	7	1879	14
1698	17	1658	12
1748	21	1783	32
1751	11	1750	15
1664	12	1616	13
1759	10	1659	12
1568	29	1452	14
1243	36	1223	12
1352	20	1295	12
1373	21	1293	12
1165	22	1068	10
1587	22	1550	14
1209	23	1197	11
1538	32	1292	13
1596	21	1542	14
1594	24	1295	14
1557	23	1333	12
1228	25	1212	11
1160	21	1145	11
1160	21	1143	11
1151	21	1143	11
1216	21	1205	11
1226	21	1137	11

1586	21	1482	14
1198	23	1140	11
1506	21	1464	14
1579	21	1475	14
1556	20	1370	13
1573	23	1385	13
1602	21	1469	14
1467	19	1365	13
1345	20	1130	11
1559	19	1403	13
1187	21	1146	11
1161	20	1154	11
1166	23	1062	10
1185	22	1053	10
1579	23	1513	14
1151	21	1065	10
1166	20	1155	11
1584	23	1538	15
2334	22	1390	14
1173	21	1137	11
1178	25	1038	10
1164	21	1159	11
1160	21	1148	11
1171	21	1153	11
1187	20	1211	11
1695	19	1583	14
2322	22	2202	19
1191	20	1209	12
1219	20	1251	12
1593	19	1564	16
1486	20	1379	12
1178	20	1169	11
1215	20	1233	10
1220	22	1161	12
1204	20	1258	11
1597	18	1563	14
1208	20	1209	11
1585	19	1549	15
1603	19	1596	13
1781	18	1759	15
1608	21	1546	13
1205	20	1198	11
1195	20	1252	12

1193	20	1221	10
1172	20	1186	11
1200	20	1179	10
1206	20	1234	11
1206	20	1212	11
1825	19	1716	13
1297	22	1177	12
1283	21	1180	10
1188	21	1152	11
1627	18	1642	15
1745	19	1703	14
1575	19	1573	13
1178	20	1165	10
1178	20	1155	10
1588	21	1592	12
1687	19	1639	15
1210	22	1140	10
1399	21	1325	11
1164	20	1141	10
1243	21	1157	10
1175	22	1246	10
1683	20	1527	12
1818	18	1582	14
1692	19	1614	16
1636	19	1613	15
1847	19	1770	18
1730	21	1675	16
1713	18	1752	16
1275	24	1141	13
1678	19	1606	17
1655	19	1775	18
1728	20	1590	17
1750	21	1722	18
1676	20	1679	16
1830	18	1743	18
1725	20	1756	18
2528	17	2534	25
1644	19	1540	16
1622	26	1360	15
1697	21	1583	14
1776	18	1799	18
1776	20	1732	18
1775	18	1770	18

1761	19	1743	18
1766	19	1656	17
1685	19	1637	17
1736	19	1538	13
1643	19	1618	17
1295	20	1261	14
1738	20	1662	16
1755	22	1054	12
1683	19	1696	17
1530	19	1502	15
1528	19	1506	16
1734	19	1714	18
1770	19	1689	17
1196	28	1186	15
1223	21	1199	13
1168	20	1203	12
1174	19	1226	12
1692	18	1593	17
1219	20	1199	13
1179	20	1176	12
1184	21	1201	12
1713	18	1743	17
1183	20	1231	12
1263	20	1172	11
1702	21	1640	17
1622	21	1553	17
1184	19	1256	13
1539	22	1596	17
1187	20	1243	13
1164	20	1288	12
1173	20	1180	13
1184	20	1217	13
1183	21	1177	13
1181	20	1222	13
1180	20	1221	12
1200	20	1170	12
1187	20	1159	12
1182	20	1176	12
1395	19	1417	15
1198	19	1251	13
1168	20	1193	13
1215	20	1172	12
1262	20	1220	12

1676	20	1645	15
1233	20	1210	12

Table 21: Curnamona Craton provenance data

Curnamona Craton	
Pb207/Pb206	$\pm 1\sigma$
1708	16
1705	15
1704	10
1623	21
1618	16
1610	16
1607	13
1607	15
1605	23
1605	17
1602	19
1602	15
1601	9
1600	8
1599	13
1597	29
1596	15
1595	13
1595	17
1594	19
1593	14
1592	11
1592	12
1589	16
1587	14
1584	17
1581	21
1581	26
1571	12
1571	17
1569	11
1568	18
1563	22
1560	24
1559	17
1558	20
1557	17

1552	16
1542	25
3242	17
1910	12
1774	15
1746	12
1725	17
1721	17
1696	13
1686	23
1667	18
1634	21
1622	17
1596	13
1595	17
1584	15
1583	20
1574	23
1574	14
1570	15
1568	18
1568	17
1567	18
1566	14
1564	22
1564	18
1563	19
1563	11
1561	11
1560	13
1560	19
1560	14
1559	20
1558	23
1556	14
1555	17
1554	21
1553	17
1552	17
1551	12
1549	13
1548	14
1546	18

1545	22
1542	38
1541	15
1540	18
1539	16
1538	18
1538	18
1538	15
1536	13
1535	12
1530	13
1528	21
1528	17
1514	18
1507	23
1504	19
1500	20
1500	29
1498	22
2786	9
2460	18
1873	12
1781	13
1776	15
1774	13
1763	16
1757	17
1744	15
1737	13
1735	16
1727	15
1718	12
1712	24
1634	12
1629	24
1628	22
1623	23
1618	17
1615	14
1614	16
1612	26
1611	34
1609	26

1607	17
1585	14
1583	26
1582	13
1578	18
1578	34
1577	22
1573	25
1573	18
1573	18
1571	22
1569	27
1554	30
1553	19
1548	21
1541	22
1608	10
1593	9
1589	14
1586	10
1585	7
1582	6
1581	13
1579	6
1577	11
1576	12
1573	8
1573	12
1571	7
1570	9
1570	7
1563	7
1562	6
1561	9
1561	5
1560	6
1560	9
1560	8
1559	11
1551	7
1549	6
1547	7
1546	10

1546	7
1546	9
1537	7
1861	12
1772	12
1707	7
1594	10
1585	22
1582	11
1571	6
1568	8
1563	6
1562	8
1550	7
1547	6
1546	6
1545	5
1544	6
1542	5
1542	7
1432	10
1318	13
1130	16
1581	8
1574	7
1572	12
1564	8
1563	7
1562	10
1556	6
1555	7
1547	7
646	7
630	7
616	8
610	7
606	8
606	7
601	6
598	8
597	8
596	8
595	8

593	8
592	8
591	6
587	8
578	7
577	7
576	7
575	7
574	8
574	7
572	7
567	7
1588	6
1588	6
1582	9
1581	3
1579	6
1578	6
1559	13
1553	8
1548	6
1544	4
1539	9
1534	4
1561	6
1559	4
1555	4
1554	3
1550	7
1549	3
1548	5
1546	4
1544	4
1544	6
1542	5
1540	6
1540	5
1540	8
1536	6
1534	4
1420	7
1306	7
1517	6

2498	13
2482	8
2472	7
2456	20
2443	12
2437	17
1874	12
1869	8
1857	10
1851	8
1830	10
1769	10
1766	12
1760	9
1758	8
1702	16
1699	12
1695	19
1695	24
1691	25
1685	12
1682	10
1674	19
1671	12
1671	9
1671	8
1663	23
1644	19
1644	15
1635	10
1629	13
1591	15
1591	31
1586	8
1584	38
1584	23
1584	17
1584	15
1583	13
1583	37
1729	10
1728	28
1726	7

1725	8
1724	10
1723	8
1721	9
1719	7
1717	23
1715	8
1714	8
1714	11
1713	8
1712	8
1711	6
1711	13
1711	10
1710	12
1708	8
1707	3
1707	9
1706	10
1706	10
1706	8
1702	9
1701	8
1696	8